SECONDARY ION EMISSION

Ya. M. FOGEL'

Khar'kov Physicotechnical Institute, Academy of Sciences, Ukrainian S.S.R.

I. INTRODUCTION

WHEN a solid surface is bombarded with a beam of primary positive ions, one observes emission from the surface of positive and negative ions, neutral particles, electrons, and electromagnetic radiation. Emission of neutral particles of the material composing the solid (cathode sputtering) and electron emission upon ion bombardment of solids are rather well-studied phenomena. There are review articles concerned with the results of studying these phenomena. The situation differs in the study of secondary ion emission. In essence, the systematic study of this phenomenon began about ten years ago, and the amount of accumulated experimental material is still small, However, as will be clear from the treatment below, the phenomenon of secondary ion emission makes possible a completely new approach to studying various physical and chemical processes at a solid-rarefied gas boundary. Hence, the systematic study of this phenomenon has acquired a great scientific and practical significance. The purpose of this article is to attract the attention of physicists and physical chemists to the as yet poorly studied phenomenon of secondary ion emission. This is because, in the author's opinion, the study of this phenomenon will not only increase understanding of processes of interaction of atomic particles with solid surfaces, but also will make it possible to use this phenomenon to study the physics and chemistry of solid surfaces.

We must give a precise definition of the phenomenon called secondary ion emission, and thus strictly define the set of problems to be treated in this article. The need of such a definition also involves the fact that sometimes the phenomenon of true secondary ion emission is confused with the reflection of primary ions from a solid surface. In secondary ion emission we are dealing with ions flying off the solid surface because momentum has been transferred from primary ions to particles existing on the solid surface. Reflection of ions is nothing other than scattering of the primary ions by the superficial layer of the solid. For this reason, the reflected ions are of the same type as the primary ions, and can differ from them only in the amount or sign of the charge. This implies that one can easily distinguish secondary from reflected ions by mass-spectrometric analysis. This is because, in all cases but one that will be treated

below, the nature of the secondary ions differs from that of the reflected ions. The only case in which it may prove difficult to distinguish the secondary from the reflected ions is when both are of the same type. This happens because the ions of the primary beam penetrate into the superficial layer of the solid, and then these occluded ions are ejected again by impact of primary ions. The reflected ions can be distinguished from the true secondary ions of the same type only when their energy distributions do not overlap. In the opposite case (which happens with primary ions of relatively low energy), one cannot make such a distinction.

The secondary ion emission must have the simplest composition in the ideal case in which the primary ion beam strikes an atomically pure surface of a solid having no bulk impurities. In this case the secondary ions will be ions of the material comprising the crystal of the solid. When the solid contains bulk impurities, the secondary ion emission will contain the ions of these impurities. Finally, the existence of a layer of adsorbed gases on the solid surface results in appearance in the secondary ion emission of ions related to the molecules of the adsorbed gases. When chemical reactions occur between the molecules of the adsorbed gases and the particles of the solid, or these molecules react with one another, the secondary ion emission will contain ions related to the products of these reactions.

The relation between the composition of the secondary ion emission and that of the particles on the surface gives us grounds for hoping that by using this phenomenon we can find a new approach to studying such surface phenomena as adsorption, catalysis, and corrosion. The first studies applying secondary ion emission to study these phenomena have given encouraging results. It is of considerable interest not only to elucidate the characteristics of secondary ion emission in order to understand the mechanism of this phenomenon, but also to study the possibilities of applying this phenomenon to study a number of surface and bulk processes of great scientific and practical significance. We should also point out that the phenomenon of secondary ion emission plays a certain role in the process of development of vacuum breakdown in various vacuum electronic devices. Contamination of the plasma in thermonuclear devices is also partially due to sputtering of secondary ions from the

walls of the chamber containing the plasma. Accordingly, this article will present the results of studies concerned only with the phenomenon of secondary ion emission and some results of applying this phenomenon to study other processes.

The systematic study of the phenomenon of secondary ion emission was started by Arnot and his associates.[1-7] The study of secondary ion emission has been renewed in the postwar period, and has been conducted mainly in the Soviet Union and the United States.

This article will present the results of the postwar studies, since on the one hand, the studies of Arnot and his associates have been treated in a series of monographs,[8,9] and on the other hand, they are quite out of date at present. The fundamental characteristics of the phenomenon will be discussed: the sputtering coefficient, the mass-spectroscopic composition and energy distribution of the secondary ions, a possible mechanism of the phenomenon, and its practical applications.

II. SPUTTERING COEFFICIENTS OF SECONDARY IONS

One of the quantities characterizing the phenomenon of secondary ion emission is the sputtering coefficient K_i of the secondary ions having a certain charge-mass ratio. This quantity is defined as the ratio of the number N_i of these secondary ions to the flux N_0 of primary ions falling on the target:

$$K_i = \frac{N_i}{N_0}.$$ (1)

We should note that the quantity K_i can depend on the value of N_0 under certain conditions in the case of secondary ions sputtered from a layer of adsorbed gases and chemical compounds on a solid surface. Hence, it can no longer be a characteristic of the phenomenon of secondary ion emission.

Let us apply the condition of adsorption equilibrium between the layer of adsorbed molecules and the gas consisting of these molecules surrounding the solid, and take account of sputtering of the molecules by the primary ion beam. Then we can derive the following for the number of secondary ions:

$$N_i = \frac{ApN_0}{Bp + C + DN_0},$$ (2)

where p is the gas pressure, and A, B, C, and D are constants.

When N_0 is small, the inequality holds that $DN_0 \ll Bp + C$, and N_i increases in proportion to N_0. That is, K_i is independent of N_0. Thus, K_i must be measured at values of N_0 having a linear $N_i = f(N_0)$ relation. As Eq. (2) implies, the value of K_i depends on the gas pressure, and this fact must be taken into account in comparing the data of measurements by different authors.

Measurement of the absolute value of K_i involves great difficulties, since on the one hand, the ions of a certain type must be distinguished from all the other secondary ions, and on the other hand, they must all be caught in some collector. In view of these difficulties, only estimates have been made up to now on the values of the sputtering coefficients of certain secondary ions.[11,12]

When a cold molybdenum target is bombarded by 600-eV Hg^+ ions, the coefficient K_i^- for the ions O^-, F^-, C^-, C_2H^-, O_2^-, and Cl^- proved to be 3, 2.5, 0.4, 0.5, 0.2, and 2%, respectively. The coefficients K_i^+ were also determined for the ions Ni^+ and Ta^+ sputtered from nickel and tantalum targets, respectively, by Cs^+ ions.[12] When the energy of the Ca^+ ions was 2700 eV, the coefficient K_i^+ for Ta^+ ions at a target temperature 1760°K was $\sim 0.6\%$. For Ni^+ ions at the same primary-ion energy and a target temperature of 1240°K, the coefficient was $\sim 0.2\%$.

Besides the coefficient K_i, we can also introduce the concept of the integral sputtering coefficient of secondary ions (sputtering yield). It is defined by:

$$K = \frac{\sum_i I_i}{I_0},$$ (3)

where $\sum_i I_i$ is the total flux of all secondary ions sputtered from the target surface, and I_0 is the flux of primary ions.

A knowledge of the values of the integral sputtering coefficients of secondary ions is necessary in constructing theories of such phenomena as vacuum breakdown and the appearance of additional ion and electron load in the accelerator tubes of cascade and electrostatic accelerators. On the other hand, the partial sputtering coefficient K_i can be calculated by multiplying the relative intensity of the corresponding mass line in the mass spectrum of the secondary ion emission by the value of the integral sputtering coefficient.*

Measurement of integral sputtering coefficients of secondary ions is also a difficult problem. The difficulty consists in the fact that sputtering of secondary ions is always accompanied by ejection of secondary electrons and reflection of primary ions. Application of a constant magnetic field to the "target-collector" system can prevent the secondary electrons from entering the collector, and thus one can measure the sum of $K^- + R$ (where K^- is the integral sputtering coefficient for negative ions, and R is the reflection coefficient of the primary ions). One can get a certain idea of the magnitude of K^- for a given measuring system under the condition $R \ll K^-$. This condition was fulfilled to some extent in[13], where they measured the value of $K^- + R$ for 200–1000 keV protons and deuterons bombarding copper, aluminum,

_____
*It is correct to define K_i in this way only when the angular distributions of all the secondary ions are the same.

and stainless steel targets. A negative flux entered the collector over this energy range, i.e., the condition R < K⁻ held. The value of K⁻ + R varied from ~ 10^{-3} at a proton energy of 200 keV to 10^{-4} at 1000 keV. When the proton energy was reduced to tens of keV, the condition R > K⁻ set in (a positive flux entered the collector), and no idea could be obtained of the value of K⁻.[14]

When a negative potential with respect to the target is applied to the collector, one can measure the quantity K⁺ + R (where K⁺ is the integral sputtering coefficient of the secondary positive ions). Such measurements have been made in[15]. However, since nothing was known in this study of the relative sizes of the coefficients K⁺ and R, again no definite information could be obtained on the value of K⁺. The same could be said of the results of[16], in which they also measured the quantity K⁺ + R for noble-gas ions of energies from 100 to 30,000 eV bombarding graphite, copper, and gold targets.

A method of measuring the values of K⁺ and K⁻ was proposed and applied in[17]. It permitted measuring these quantities in the presence of secondary electron emission and reflection of primary ions. By this method they measured the coefficients K⁻, K⁺, and R for Mo targets bombarded by H⁺, He⁺, Ne⁺, Ar⁺, Kr⁺, and O⁺ ions of energies from 10 to 40 keV, and for Ta, W, Cu, and Fe targets bombarded by H⁺, Ne⁺, and Ar⁺ ions of the same energy range.

Figure 1 gives the curves for K⁻(v), K⁺(v), and R(v) (where v is the ion velocity) for all the metals studied in[17].

Some information on the value of the coefficient K⁻ for bombardment of a series of alkali-halide crystals by Li⁺ and K⁺ ions is to be found in[18,19]. The sec-

ondary ions were sputtered from the crystal surface with single pulses of primary flux of several microseconds duration. On the one hand, bombardment of the crystal in a single-pulse system avoided charging of the surface, and on the other hand, it permitted distinguishing the secondary negative ions from the electrons by their times of flight from the target to the collector. The mass of a negative ion could be estimated from its time of flight. Cl⁻ ions were sputtered from NaCl and KCl crystals, Br⁻ ions from KBr, and F⁻ ions from NaF. The sputtering coefficients of these ions for an energy of the primary K⁺ ions of the order of 1 keV amounted to 7–10%.

III. THE MASS SPECTRUM OF SECONDARY ION EMISSION

Mass-spectrometric studies of the composition of secondary ion emission have been made in[1-6,11,13,16,20-32]. These studies have shown that the composition of the secondary positive and negative ions depends on the following factors:

1) The nature of the target.

2) The nature, energy, and current density of the primary ion beam.

3) The temperature of the target.

4) The composition and pressure of the gas surrounding the target.

While the experimental conditions in the studies discussed below could not ensure that all the factors cited above remained identical, and hence the results of different authors do not agree in a number of cases, still we can draw some general conclusions from these results.

First of all, we can state that the secondary positive and negative ion emission contains:

1) Ions of the target material itself.* The origin of these ions can vary. They can be sputtered from the target material itself, or from chemical compounds on its surface.

2) Ions of a bulk impurity in the target material.

3) Ions of the same type as those in the primary beam.

4) Ions of molecules of chemical compounds occurring on the surface of the target, or fragments thereof.

5) Ions of molecules adsorbed on the surface of the target, or their fragments.

As an example bearing out this conclusion on the composition of secondary ion emission, we can give the data of a mass-spectrometric analysis of particles sputtered from an Ag surface by impact of 400-eV Xe⁺ ions, as obtained in[20] (see Table I).
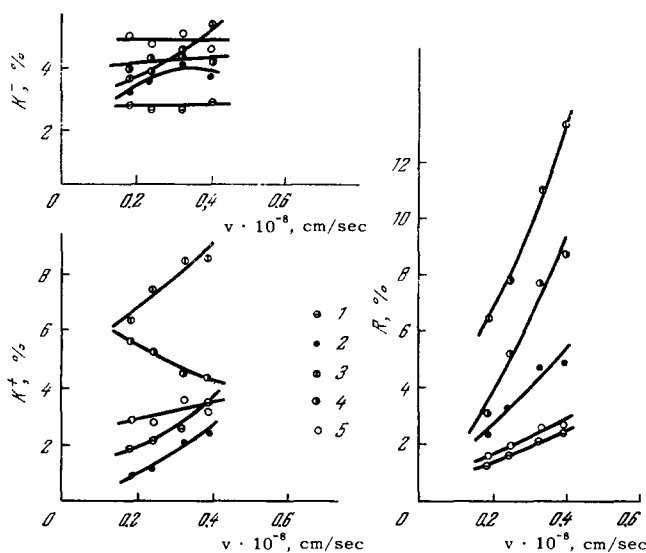
A mass-spectrometric analysis was made in this

FIG. 1. The functions K⁺(v), K⁻(v), and R(v) for various metals. Primary ions: 1 — Mo; 2 — Fe; 3 — Ta; 4 — W; 5 — Cu.

*Naturally, one can observe negative ions of the target material only when they are stable, or if they are metastable, they have lifetimes greater than their time of flight to the mass spectrometer.

Table I.

Mass	Neutral particles		Positive ions		Negative ions	
	Form	Intensity	Form	Intensity	Form	Intensity
1					H^-	W
15			CH_3^+	W		
16					O^-	S
17					OH^-	S
18	H_2O	S	H_2O^+			
19					F^-	M
23			Na^+	VS		
24			Mg^+	S	C_2^-	M
25			Mg^+, C_2H^+	S	C_2H^-	M
26	C_2H_2	M	$Mg^+, C_2H_2^+$	S	$C_2H_2^-$	S
27			$Al^+, C_2H_3^+$	M	$C_2H_3^-$	W
28	CO	S	$C_2H_4^+$	W		
29			$C_2H_5^+$	M		
32			S^+	W	S^-	M
33					SH^-	M
34					SH_2^-	M
35					Cl^-	S
37					Cl^-	S
39			K^+	VS		
40			Ca^+	M		
41			K^+	S		
42			$C_3H_6^+$	M		
43			$C_3H_7^+$	M		
44	CO_2	M	$CO_2^+(?)$	M		
45					(?)	W
48					C_4^-	W
49					C_4H^-	W
50	C_4H_2	W				
51	C_4H_3	W				
52	C_4H_4	W	$C_4H_4^+$	W		
54			Fe^+	W		
56			Fe^+	W	(?)	W
57			$C_4H_9^+$	W	(?)	M
58			$C_4H_{10}^+$	W	(?)	W
59					(?)	M
60					(?)	W
62—68			Xe^{++}	S		
70			(?)	W		
75			As^+	W	(?)	M
76					(?)	M
77					(?)	W
78			$C_6H_6^+$	W	(?)	W
80			(?)	W		
82			(?)	W		
92			$C_5H_5CH_3^+$	W	(?)	W
98					(?)	VW
107			Ag^+	S		
108					$AgH^-(?)$	M
109			Ag^+	S		
110					$AgH^-(?)$	M
124—136			Xe^+	VS		
160						
185			W^+ or Ta^+	M		
198—204			Hg^+	S		
214—218			Ag_2^+	S	Ag_2^-	M
230—234			Ag_2O^+	W	Ag_2O^-	S
246—250					$Ag_2O_2^-$	W
321—327			Ag_3^+	W		

The conventional symbols for the intensity values are: VS — very strong; S — strong; M — medium; W — weak; VW — very weak.

study not only of the charged but also the neutral particles sputtered from the target. In order to analyze the neutral particles sputtered from the target, they were ionized by an electron beam. The residual gas pressure in the target chamber was 10^{-7} mm Hg. When the noble gas was admitted into the ion source of the apparatus, the pressure in the target chamber rose to 10^{-4} mm Hg.

As we see from Table I, the mass spectrum of the Ag target contains secondary ions of the five groups listed above.

Study of the mass spectrum of secondary ions from targets made of Al,[16] Fe[16,31] Cu,[13,16,24] Ge,[20] Mo,[21,23] Nb,[32] Ta,[16,21,27] W,[16] and Pt[16,22,29,30] has shown that the mass spectrum of these targets consists of the same groups of ions as in the mass spectrum of Ag. However, the relative amounts and types of ions contained in these groups vary for different targets. These variations involve both the change in the nature of the target itself and the change in the composition of the film of adsorbed gases and chemical compounds on the surface. With the composition of the residual gas remaining unchanged, the composition of this film varies with the nature of the
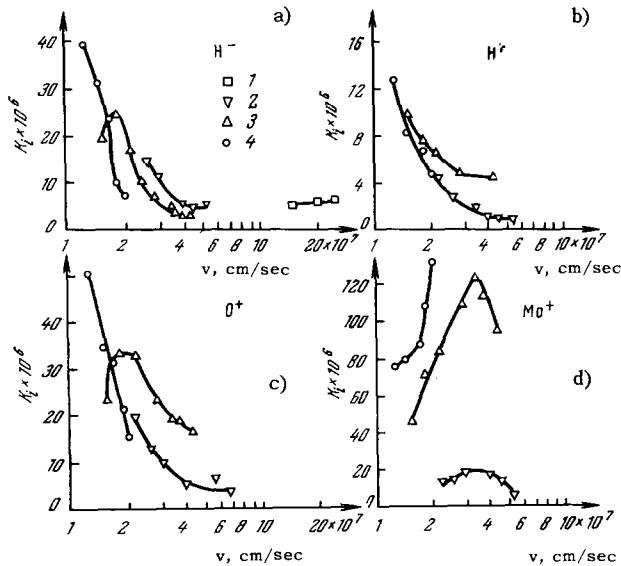
FIG. 2. The functions $K_i(v)$ for the secondary ions H^-, H^+, O^+, and Mo^+. Primary ions: $1 - H^+$; $2 - Ne^+$; $3 - Ar^+$; $4 - Kr^+$.

target. This results from changes in the rate of adsorption of the components of the residual gas onto the target surface, and from changes in the nature of the chemical interaction of the residual gases with the target material.

In [23] the relation between the number of sputtered secondary ions and the velocity and nature of the primary ions was studied. Figure 2 shows the $K_i(v)$ curves* for certain secondary ions sputtered from a molybdenum target.

An interesting feature of the $K_i(v)$ curves in the velocity range $v > v_{max}$ is the gradual decline in the slope of the curve with increasing velocity. It gives the impression that when $v \gg v_{max}$, the number of sputtered ions ceases to depend on the velocity of the primary ion, and approaches a constant value. Such a velocity-independence of K_i is actually observed for the pair $H^- - H^+$ (see Fig. 2a) in the velocity range of $\sim 2 \times 10^8$ cm/sec. An analogous situation also occurs when negative ions of molybdenum oxides are sputtered by Ar^+ ions.

The course of the $K_i(E)$ curves in the region $E \gg E_{max}$ (E_{max} is the energy corresponding to the maximum on the $K_i(E)$ curve) agrees rather well with the formula $K_i \sim (\ln E)/E$ derived in [33] for the sputtering coefficient of metals by high-energy ions.

In the region $E < E_{max}$, the course of the $K_i(E)$ curves has been studied in [11, 21]. They established that there is a threshold energy for the primary ions. Primary ions of energies below the threshold no longer eject secondary ions from the target. In this

respect, the phenomenon of secondary ion emission also manifests an analogy with sputtering of metals by ion impact, which is characterized by the existence of a threshold energy. The size of the threshold energy can be characterized by the following numbers taken from [21]. For the secondary ion-primary ion pair Mo^+-Ar^+ (Mo target), it is 80 eV, and 60 eV for the pair Ta^+-Ar^+.

Of course, the observed analogy gives no grounds for stating that cathode sputtering and secondary emission of ions of the target material are two aspects of the same phenomenon. To justify such a statement, further studies are needed on both phenomena under conditions of atomic purity of the target surface (see below).

The composition of the mass spectrum of the secondary ions depends on the current density of the primary beam. At high current densities, the target surface is cleaned of molecules of adsorbed gases and surface compounds, and the groups of secondary ions involving these molecules must disappear from the mass spectrum. This phenomenon has been observed in [26] when various targets were bombarded with an ion beam of energy 10 keV and current density 20 microamperes/mm^2. At this current density, the mass spectra of Mg and Ti targets showed only the secondary ions of the target materials themselves, namely Mg^+, Mg^{++}, Mg_2^+, and Ti^+, Ti_2^+, respectively.

We must make the following remark on the results of [26]. As Eq. (2) implies, the number N_i of secondary ions approaches a constant value as the number N_0 of bombarding primary ions increases. This conclusion is valid under the condition that the rate of adsorption or the rate of reactions forming surface chemical compounds is independent of N_0. If N_i is observed to decrease beyond a certain value of N_0 on the curve of the relation $N_i = f(N_0)$, this means that the rate of the processes indicated above decreases with increasing N_0. With further increase in N_0, the target surface can attain a state in which N_i declines to experimentally undetectable values. That is, certain ions disappear from the mass spectrum of the secondary ion emission. The author of [26] has attained such values of the current density of the primary beam for Mg and Ti targets.

The temperature of the target substantially affects the mass spectrum of the secondary ions. As a rule, the intensity I of the beams of secondary ions involving the presence of adsorbed molecules on the target surface declines monotonically with increasing target temperature. At a certain temperature, depending on the nature of the secondary ion, the value of the beam intensity becomes so small that it can no longer be measured by the apparatus detecting the secondary ions. Such a course of the $I(T)$ curves for the secondary ions involving adsorbed molecules is evidently due to an increase in the rate of desorption of these molecules with increasing target tem-

---

*In this case the quantity K_i represents the ratio of the secondary ion flux at the mass-spectrometer collector to the primary ion flux at the target.
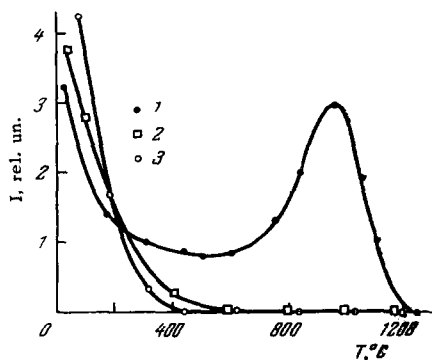
FIG. 3. The relation of the line intensity of the secondary ions C_2^-(1), C_2H^-(2), and $C_2H_2^-$(3) to the temperature of platinum in a residual-gas atmosphere.

FIG. 4. Mo target, primary Ar^+ ions. a) $K_i(T)$ curves for Mo^+ ions: 1, 2 — data of[23]; 3, 4 — data of[21]; b) $K_i(T)$ curves for ions of molybdenum oxides: $\triangle$ — MoO_3^-, $\square$ — $Mo_2O_3^-$, $\bullet$ — MoO_2^-.

perature. However, in some cases the decline in emission of the observed secondary ions with increasing target temperature is not monotonic. One of these cases is illustrated in Fig. 3, which has been taken from [30]. This diagram shows the I(T) curves for the C_2^-, C_2H^-, and $C_2H_2^-$ ions ejected from a Pt surface. This decline in intensity is due to the decrease in the covering of the Pt surface by the molecule from which the C_2H^- and $C_2H_2^-$ ions are ejected, owing to their desorption or thermal decomposition. The non-monotonic course of the I(T) curve for C_2^- ions can be explained if we bear in mind the possibility that free carbon can be formed on the Pt surface by cracking of adsorbed hydrocarbon molecules contained in the residual gas. The course of the I(T) curve for C_2^- ions can be understood if we take into account the fact that C_2^- ions can be sputtered both from molecules of adsorbed hydrocarbons and from free carbon. Above 600°C, where the covering of the Pt surface by adsorbed hydrocarbon molecules becomes very small, to judge from the I(T) curves for the ions C_2H^- and $C_2H_2^-$, the C_2^- ions are mainly sputtered from free carbon. The formation of free carbon on the heated Pt surface was confirmed by experiments in which oxygen was admitted into the target chamber.[30]

The disappearance or substantial weakening, with increasing target temperature, of the emission of secondary ions that involve the covering of the target surface with molecules of adsorbed gases has also been observed in [23,28,32,34].

The intensity of the secondary-ion beams sputtered from molecules existing on the target surface of chemical compounds of the metal atoms with particles of the residual gas also depends on the temperature. The nature of the $K_i(T)$ and I(T) relations for these ions can be seen from Figs. 4 and 5, which give the corresponding curves for the Mo^+ ion, the negative ions of the oxides of molybdenum, and the positive ions of the niobium oxides, as taken from [21,23,32].
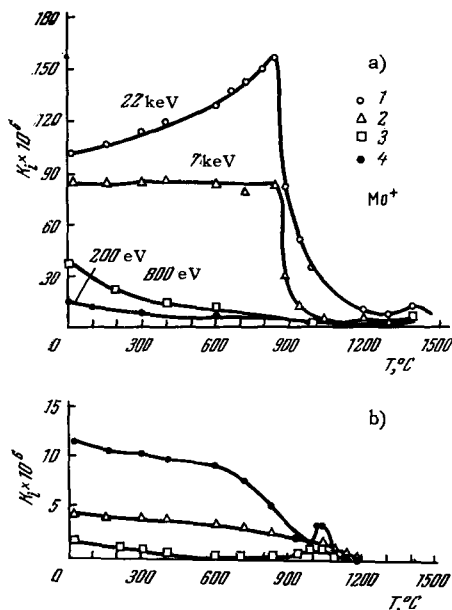
The course of the curves in Figs. 4 and 5 is due both to thermal decomposition of the oxides on the target surface, with changeover from some forms of oxides to others, and to evaporation into the gas phase. The latter process was clearly marked with Nb, for which it was established by ionizing the gas phase with electrons that the oxide NbO evaporates into the gas phase at temperatures above 1500°C.[32]

If we examine the curves in Figs. 4 and 5, we can easily show that the ions of the metal itself are sputtered mainly from the oxides on its surface. In fact, when the covering of the surface of Mo becomes very small at temperatures above 1200°C (emission of the ions $Mo_2O_3^-$, MoO_3^-, and MoO_2^- disappears), the emission of Mo^+ ions also is decreased manyfold (see Fig. 4). The analogous shape of the curves for the ions NbO^+ and Nb^+ allows us to state that the Nb^+ ions are mostly sputtered from the oxide NbO. The author of [21] concluded that Ta^+ ions are not sputtered from the crystal structure of the metal itself, but from a nitride on its surface, on the basis of the identical shape of the curves for the Ta^+ and TaN^+ ions. We should note that after the target surface has been cleaned of chemical compounds, the intensity of the beam of metal ions sputtered from the crystal no longer is temperature-dependent.

The effect of the temperature on the emission of secondary ions involving the covering of the target surface with molecules of chemical compounds has also been studied in [27,28,31].

Since the gaseous medium surrounding the target is in dynamic equilibrium with the film of adsorbed molecules on the target surface, its composition and
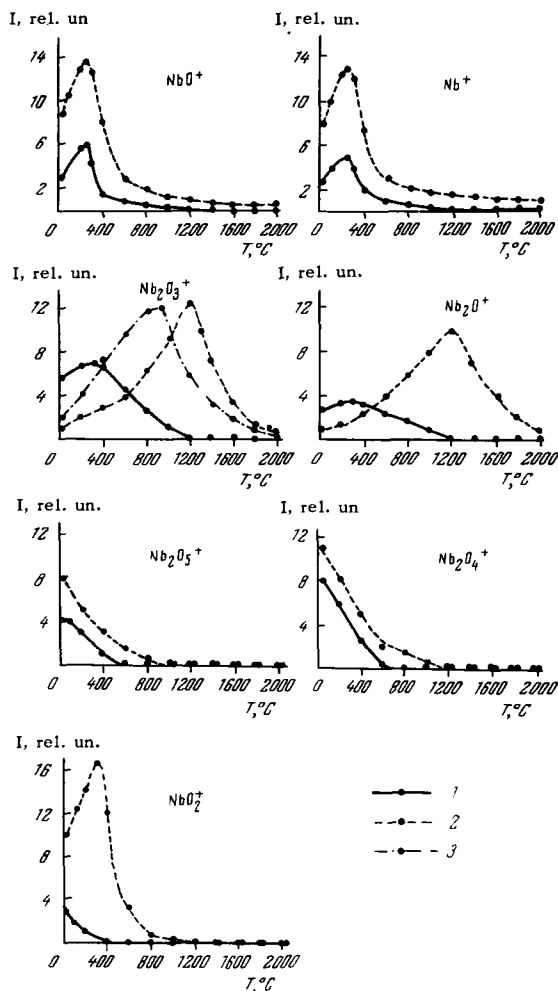
FIG. 5. The functions I(T) for the secondary ions Nb^+, NbO^+, Nb_2O^+, $Nb_2O_3^+$, $Nb_2O_4^+$, and $Nb_2O_5^+$. 1 — niobium strip in a residual-gas atmosphere; 2 — niobium strip in an oxygen atmosphere ($p = 5 \times 10^{-5}$ mm Hg); 3 — niobium strip in an oxygen atmosphere ($p = 3 \times 10^{-5}$ mm Hg).

pressure must exert a considerable influence on the mass spectrum of the secondary ion emission. This influence was first found in [23] in a study of the action of D_2O vapor on a molybdenum surface.

The Mo target was heated to 1500°C in residual gas. Then D_2O vapor was admitted into the target chamber to a pressure of 10^{-4} mm Hg. The target was cooled in the atmosphere of D_2O vapor to room temperature, and the mass spectrum of the secondary ion emission was studied at this temperature. Figure 6 shows the spectrum of the negative ions from the Mo target in the residual-gas atmosphere and in D_2O vapor. As we see from Fig. 6, the action of the D_2O vapor on the target brings about appearance of the ions OD^- and D^- in the mass spectrum. D^+ ions appear in the positive-ion spectrum. Thus we can state that the adsorption of D_2O vapors onto the target surface gives rise to the ions OD^-, D^-, and D^+ in the mass spectrum. The conclusion from this is that the
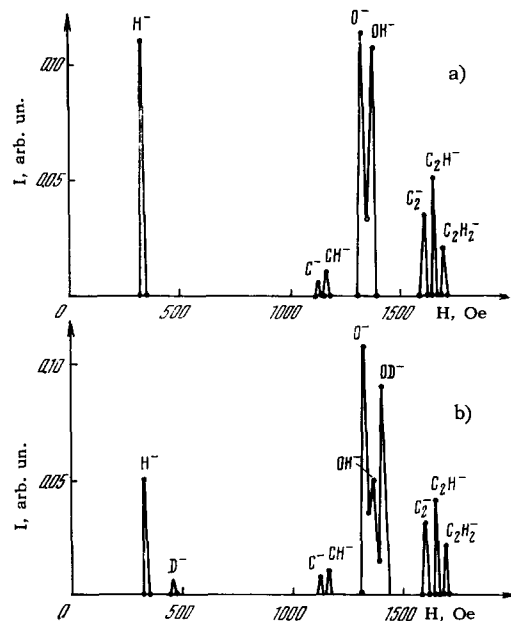

FIG. 6. Mass spectrum of negative ions from an Mo target in a residual-gas atmosphere (a) and in a D_2O-vapor atmosphere (b).

ions H^-, H^+, and OH^- arise from the presence of H_2O molecules on the target surface. As for the ions H^- and H^+, we can state that they come not only from H_2O molecules, but also from some other hydrogen-containing molecule. This conclusion follows from comparing the peak heights of H^- and OH^- in Fig. 6a with those of D^- and OD^- in Fig. 6b.

An experiment analogous to that described was performed in [34]. D_2O vapor was adsorbed onto a Be surface, and the same results were obtained.

Figure 7 shows a typical curve illustrating the effect of the gas pressure on the beam intensity of the secondary ions, involving its action on the target. The shape of the $K_i(p)$ curve agrees with Eq. (2).

The profound effect on the nature of the secondary-ion mass spectrum of such factors as the target temperature and the nature of the gas surrounding it makes it possible to apply the phenomenon of secondary ion emission to study various surface processes (adsorption, catalysis, gaseous corrosion) due to the interaction of gases with solid surfaces (see below).
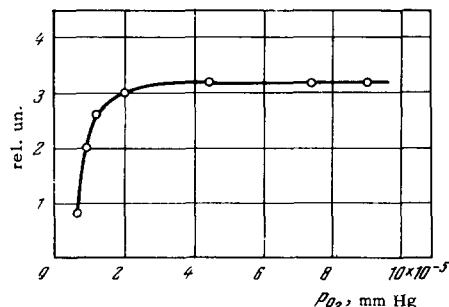

FIG. 7. The $I(P_{O_2})$ curve for secondary Na_2O^+ ions sputtered from a platinum target in an oxygen atmosphere.

IV. THE ENERGY DISTRIBUTION OF SECONDARY IONS

From the standpoint of elucidating the mechanism of the phenomenon of secondary ion emission, it is important to know the distribution of initial energies of the secondary ions. Knowledge of this distribution is also of practical importance, since the degree of monokineticity of the secondary ions determines the resolving power of the ion microscope, which is based on secondary ion emission (see below). The information accumulated up to now on the initial energies of secondary ions, as obtained in [20-22,36-41], is presented below.

First we should note that one can gather valuable information only from energy distributions obtained from a secondary ion beam that is homogeneous in composition, in view of the varying origin of the secondary ions comprised in the groups discussed in Chapter III. Hence, in all the studies concerned with energy distributions of secondary ions, except [39], these distributions were studied on secondary ions that were homogeneous in composition, as isolated by a magnetic analyzer.

The energy distribution of secondary ions has been studied in different ways: by the retarding-field method, [20,22,35,40,41] by studying the curve profile for the relation of the secondary-ion current at the mass-spectrometer collector to the magnetic field intensity of the analyzing electromagnet, [21,37] by determining the resolving power of an ion microscope forming an image with the secondary ions, [36] and finally, by using a cylindrical electrostatic analyzer. [38,39]

Figure 8 shows the curve for the energy distribution of secondary Mo$^+$ ions. The half-width of the energy distribution of the Mo$^+$ ions proved to be 30–35 eV.* The energy distribution extends to energies above 100 eV. The energy distribution of secondary ions sputtered from a beryllium target was studied in [38]. Figure 9 shows one of these curves for K$^+$ ions sputtered by 1000-eV Ar$^+$ ions. The curve was taken at an energy resolution of the electrostatic analyzer of 0.8 eV. The same diagram shows the energy distribution curve of the Ar$^+$ ions arising in the argon that had entered the target chamber from the ion source. As the author suggests, the Ar$^+$ ions were formed by charge-transfer from the primary ions in the argon. As we see from Fig. 9, the energy distributions of the K$^+$ and Ar$^+$ ions differ from one another substantially, both in the half-width of the distributions, and in the values of the peak and most-probable energies. K$^+$ ions are observed at energies even above 30 eV, while there are no Ar$^+$ ions of energies above 5 eV.

---

*The half-width of an energy-distribution curve is defined as the width in energy units of this curve at a height equal to half the peak intensity.
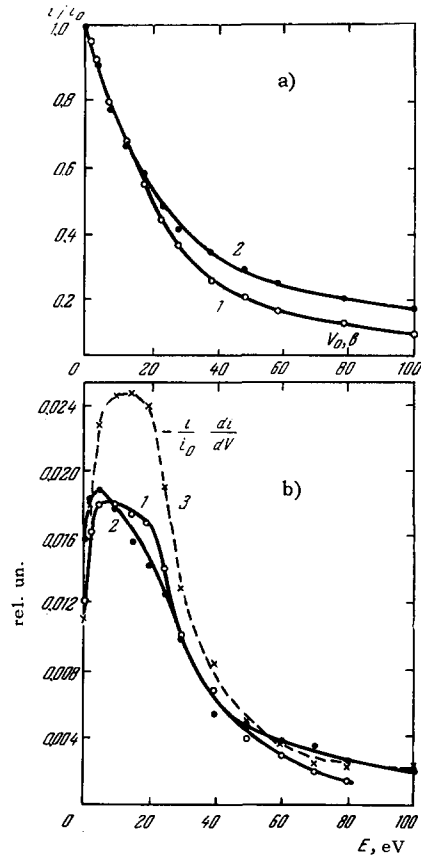

FIG. 8. Retardation curves (a) and energy spectra (b) of sputtered Mo$^+$ ions (T = 1800°K); curve 1: U = 900 eV; curve 2: U = 2150 eV; curve 3: U = 900 eV (without correcting for the transmission of the mass spectrometer).

A substantial difference was observed in [40,41] between the energy distributions of the secondary ions of the main metal (Be$^+$ ions) and those of an impurity (K$^+$ ions). Here they studied the energy distributions of various secondary ions sputtered from Al, Mg, and duraluminum by Hg$^+$ ions of energies from 200 to 2000 eV. Figures 10 and 11 show the energy distributions of a number of secondary ions sputtered by 1800-eV Hg$^+$ ions from duraluminum. As
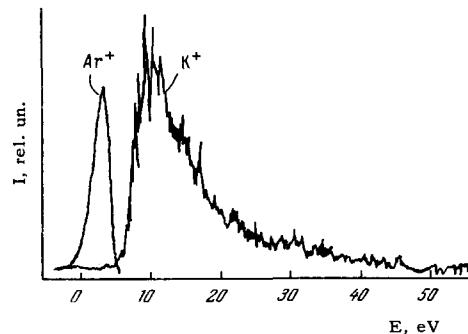

FIG. 9. Energy distributions of secondary K$^+$ ions sputtered from Be by 1000-eV Ar$^+$ ions.

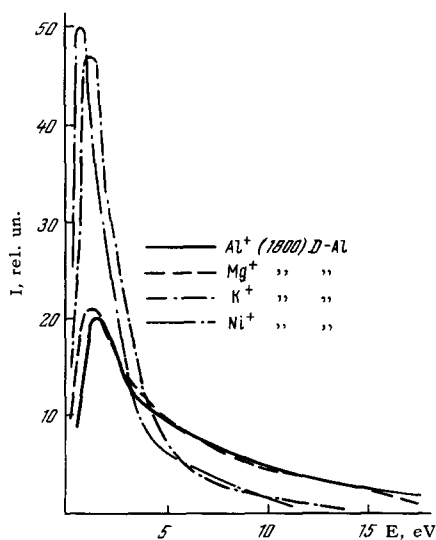FIG. 10. Energy distributions of secondary Al^+, Mg^+, K^+, and Ni^+ ions sputtered from duralumin by 1800-eV Hg^+ ions.

we see from these diagrams, the energy distribution of the Al^+ ions has a greater half-width and extends to higher energies than those of impurity ions (K^+ and Ni^+ ions), those of chemical compounds ($AlOH^+$ ions), or those involving adsorbed molecules (H_2O^+ ions). The same is true for Al^+, Na^+, and K^+ ions sputtered from Al(99.99%).

An effect of the primary-ion energy on the nature of the energy distribution of the secondary ions was established in [41]. As the primary-ion energy was increased, the most-probable energy of Al^+ ions sputtered from Al (99.99%) is shifted to higher energies. The half-width of the energy-distribution curve
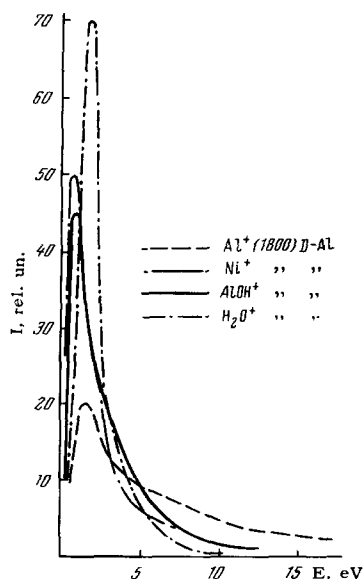

FIG. 11. Energy distributions of Al^+, Ni^+, $AlOH^+$, and H_2O^+ secondary ions sputtered from duralumin by 1800-eV Hg^+ ions.

is 6 eV for an Hg^+-ion energy of 200 eV, but increases to 13.5 eV at an energy of 2000 eV.

One can study the energy distribution of sputtered atoms by ionizing the atoms ejected from the target by an electron beam. Such a study was made in [41] for Al atoms. It turned out that the energy distributions of the Al atoms and the Al^+ ions sputtered from an aluminum target did not differ substantially from one another.

In view of the paucity of studies concerned with energy distributions of secondary ions, it is still too early to draw any general conclusions on the effect of various factors (the energy and nature of the primary ions, the nature and temperature of the target, the type nature of secondary ions, etc.) on the nature of the distribution. However, the results obtained permit us to state some conclusions on a possible mechanism of the phenomenon of secondary ion emission. This will be discussed in the next section of this article.

V. ON THE MECHANISM OF SECONDARY ION EMISSION

The development of a theory of secondary ion emission must be based on definite conceptions of the mechanism of this phenomenon. Having such conceptions will make it possible to give a correct treatment to the results of studies in which this phenomenon is applied to study various processes on solid surfaces in a rarefied gas (see below). The question arises of whether the data presented in the previous sections of this article suffice for definite conclusions on the mechanism of secondary ion emission, or whether further studies are needed, directed toward elucidating this mechanism. In discussing this problem, as we see it, the general considerations stated below are of considerable importance.

In order to formulate a definite conclusion on the mechanism of secondary ion emission, we must answer two primary questions:

1) What processes accompanying collision of the primary ion with the solid surface are responsible for the fact that the secondary ion acquires the energy and momentum with which it leaves the solid surface to enter the surrounding rarefied gas?

2) What processes determine the charge of the parting ion?

We should note at the outset that the mechanisms of emission of different secondary ions can differ. This remark involves the fact, as noted above, that secondary ions are sputtered both from the crystal structure of the target or from bulk impurities contained within it, and from chemical compounds or adsorbed gases on the target surface. Therefore, even secondary ions of the same type can have a different emission mechanism, depending on whether they are sputtered from the crystal structure of the target or from chemical compounds on its surface.

In discussing the problem of the mechanism of secondary ion emission, we can compare this phenomenon with the simpler and somewhat related phenomenon of cathode sputtering. Such a comparison can prove useful, since the characteristics of the phenomenon of cathode sputtering have been studied rather well, and attempts have been made to treat this phenomenon theoretically.

It makes very good sense to compare cathode sputtering of the target with emission of secondary ions of its substance. However, such a comparison can lead to definite conclusions only when the surface of the target is clean enough. In the converse case, it is possible that in cathode sputtering not only atoms of the target will be sputtered, but also molecules of chemical compounds occurring on its surface.* On the other hand, when the target surface is not clean enough, ions of the target substance can be sputtered both from its crystal structure and from surface compounds. Only when the target is cleaned of surface compounds will both the atoms and the ions be sputtered from the crystal structure.

The theory of cathode sputtering deals with a mechanism of relay energy transfer from the primary ion to the atom of the crystal that flies off into the vacuum. According to this notion, the primary ion penetrates within the crystal structure of the solid, and transmits momentum to its atoms. These atoms, which are arranged at the sites of the structure, in turn transmit momentum to other atoms. Thus, finally, the momentum reaches the surface of the solid by relay transfer, and is transmitted to an atom on the vacuum boundary. If the surface atom acquires enough momentum to remove it from the crystal, it will fly off into the vacuum. That is, an elementary cathode-sputtering event will take place. A number of peculiarities of this phenomenon have been explained on the basis of the discussed mechanism of cathode sputtering. These include the anisotropy of direction of flight of the sputtered atoms. This is observed when single crystals are sputtered with ion beams, and involves momentum transfer in the crystal along close-packed directions (focused collisions).[43]

It is of interest to compare the results of experimental studies of cathode sputtering and secondary ion emission with the conclusions of the theory based on the relay momentum-transfer mechanism. As was stated above, such a comparison will lead to definite conclusions only when both phenomena are studied on targets with clean surfaces. In this case, study of the relation of the sputtering coefficients of atoms and ions to the primary-ion energy and the temperature of the monocrystalline target, comparison of the energy distributions for atoms and ions, determination

of the threshold energies for both processes, and determination of the nature of the directional anisotropy of the sputtered atoms and ions will make it possible to determine whether the mechansims of momentum transfer from primary ions to target atoms and ions are the same or different. If they prove to be the same, then the conclusions from the theory of cathode sputtering can be applied also to the phenomenon of secondary emission of ions of the crystal. Experiments under the conditions stated above are very difficult, and have not been performed yet.

The emission of secondary ions involving the existence on the solid surface of adsorbed molecules and molecules of surface chemical compounds can also be considered to be the sputtering of these molecules by the ions of the primary beam. Perhaps the emission of the stated ions, as well as that of certain others, results not only from relay momentum transfer, but also from binary collisions of the primary ions with molecules on the solid surface. The possibility of binary collisions of primary ions with atoms of the solid surface is indicated by experiments on scattering of ion beams by solid surfaces.[44–46]

Binary interaction with the metal surface results in sputtering both of ions corresponding to an unfragmented adsorbed molecule or one of a surface chemical compound, and of ions of dissociation products of these molecules. (For example, we can cite the emission of the ions $Fe(CO)_5^+$, $Fe(CO)_4^+$, $Fe(CO)_3^+$, $Fe(CO)_2^+$, and $Fe(CO)^+$, observed when the compound $Fe(CO)_5$ is formed on the surface of iron,[31] or the emission of the ions NH_3^+, NH_2^+, NH^+, H_2^+, H^+, and N^+ from the surface of platinum in an ammonia atmosphere.[30]) In this case the sputtering of the secondary ions can be treated by analogy with the dissociative-ionization processes that occur in collisions of ions with molecules of rarefied gases.[47,48] In secondary ion emission, the primary ions ionize adsorbed molecules, with part of the ionized molecules decomposing into fragments. If in this process the molecular ion and its fragments acquire enough kinetic energy to eject them from the metal surface, then the corresponding secondary ions will be emitted. Analogously, emission of secondary ions can involve molecules of surface chemical compounds. The difference from the case of adsorbed molecules will consist only in the fact that, when ions of surface compounds containing atoms of the metal fly off, they do work against the binding forces of the atoms to the metal crystal, rather than against adsorption forces, as when ions of adsorbed molecules fly off.

In order to determine which of the variant types of momentum transfer to a particle on the solid surface is involved in the emission of any particular secondary ions (relay or binary interaction), it is desirable to perform the experiments by comparing the secondary ion emission under identical conditions from

---

*Sputtering of molecules of chemical compounds of target atoms by primary-ion impact has been observed in [20,42].

massive targets and from targets of the same material, but taken in the form of a very thin free film. Experiments on comparative study of the dissociative-ionization and secondary ion emission spectra in collisions of ions with the molecules of a gas in the free and adsorbed states would be very useful in solving this problem.

A mechanism of secondary ion emission not involving processes of momentum transfer from a primary ion to a particle on the solid surface has been proposed in [49]. The authors of this study start from the idea that secondary electron emission occurs when the solid surface is bombarded by primary ions. In their opinion, the emission of secondary ions results from collision of the secondary electrons with molecules of gases adsorbed on the surface of the solid.

We shall now go on to discuss the factors determining the charge of the particles ejected from the solid surface. These factors are the initial charge of the particle on the surface, the process by which energy is transferred to it, and the conditions of electron exchange as it leaves the surface.

We shall first take up the very simple case of sputtering of secondary ions from the crystal of a metal having an atomically-clean surface. In this case, a positive ion of the metal is ejected, and it can capture an electron as it leaves the surface of the metal, and thus fly off as an atom. In the equilibrium evaporation of ions, the ratio n^+/n^0 (where n^+ and n^0 are the number of particles evaporating from the surface in the positive and neutral charge states) is determined by the well-known Saha-Langmuir formula. According to the data of [12], the value of n^+/n^0 in the ejection of the secondary ions Ta^+ and Ni^+ by Cs^+ ions proves to be 10^7–10^9 times greater ($n^+/n^0 \approx 10^{-2}$) than that calculated by the Saha-Langmuir formula. The inapplicability of the Saha-Langmuir formula to calculate n^+/n^0 for secondary ion emission involves the fact that the process of ejecting secondary ions is thermodynamically a non-equilibrium process. The large value of n^+/n^0 in sputtering of secondary ions is explained by the fact that their velocities are much greater than thermal, and as has been shown in [50], the probability that an ion will capture an electron as it leaves the surface of the metal declines as its velocity increases.

The emission of negative ions from the structure of the metal, as observed in [25,28,29,31], involves the existence on the surface of chemical compounds of atoms of the metal with molecules of the surrounding gas atmosphere. This statement is confirmed by the fact that emission of negative ions decreases when the metal is heated, and disappears at a certain temperature. At the same time, the emission of secondary molecular ions involving the existence of chemical compounds on the metal surface also disappears. Estimates show that the value of n^-/n^0 for secondary

emission of negative ions of the metal itself, as well as for other negative ions, is much greater than that calculated by the Saha-Langmuir formula for equilibrium evaporation. Apparently the reason for this involves the fact that the probability that a negative ion will lose its extra electron while flying off the metal surface declines considerably with increasing velocity.

While discussing the problem of the charge state of secondary ions as involving existence on the solid surface of molecules of adsorbed gases and surface chemical compounds, we should treat separately the emission of fragmentary ions and of the ions of the unfragmented molecule. If the original molecules are in the neutral state, then the fragmentary positive and negative ions can arise, as was stated above, in collisions with secondary electrons or in binary collisions with the primary ions. The formation of these ions, especially the negative ones, is less probable in relay momentum transfer.

The conditions differ in the emission of ions corresponding to the unfragmented molecule. In this case the possibility is ruled out that they could be formed by collisions of secondary electrons with the original molecules. Positive ions of this type can arise by transfer of momentum to the original molecule by the relay mechanism or by binary collisions with primary ions. As for the negative ions of the unfragmented molecule, they can arise in only one way. Namely, they can arise by relay momentum transfer to an original particle existing on the surface in a negatively-charged state. Thus, the very fact of emission of molecular negative ions of this type will indicate that these ions exist on the surface of the metal.*

As we see from what has been said in this chapter, the mechanism of emission of the various secondary ions is still not clear. Extensive and many-sided experimental studies are needed to elucidate it. It will then become possible to create a theory of secondary ion emission.

VI. ON SOME APPLICATIONS OF THE PHENOMENON OF SECONDARY ION EMISSION

a) Use of the Phenomenon of Secondary Ion Emission to Study Catalytic and Corrosion Processes

As we see from what has been said in the earlier sections of this article, study of the phenomenon of secondary ion emission is just beginning. However, the existing information on this phenomenon lays a groundwork for studying the possibilities of applying it, mainly to the study of processes occurring in the layer of adsorbed molecules and molecules of chem-

---

*The possible existence of negative ions on the surface of a metal, e.g., O_2^-, is important in treating certain catalytic processes.

ical compounds on a solid surface.*

Processes occur in the surface layer that are of great practical importance. Above all, these include the heterogeneous catalytic reactions. The initial stage of gaseous corrosion is the formation of surface chemical compounds. To obtain an ultrahigh vacuum and a pure hydrogen plasma in thermonuclear fusion devices involves processes of adsorption and desorption occurring in the surface layer of the solids in contact with the gas.

Some observations described in Chapter III of this article, which was devoted to the mass spectrum of secondary ion emission, give grounds for stating that changes in the condition and composition of the surface layer of a solid are reflected in corresponding changes in the mass spectrum of the secondary ions sputtered from the surface of this solid. The notion thus arises of processes occurring in the surface layers of solids could be studied by observing the changes in the mass spectrum of their secondary ion emission due to the occurrence of these processes. Naturally, the information on the surface processes will be more complete if the study of the secondary ion emission mass spectrum is combined with study of the mass spectrum of the ions obtained by ionizing the gas phase by an electron beam. A new method has been based on observing the shape of the $I(T)$ and $I(p)$ curves (where I is the intensity of a certain line in the mass spectrum, T is the temperature of the solid, and p is the gas pressure) for the secondary ions sputtered from the solid surface by a primary-ion beam, and that of the $I(T)$ curves for the ions obtained by ionizing the gas surrounding the solid. The present author and his associates have applied it to study a number of catalytic, adsorption, and corrosion processes.[28,30-32,51-55]

These processes were studied in an apparatus described in detail in [30]. As an example of application of the secondary ion emission method† to study catalytic processes, the results are presented below of a study of the decomposition and synthesis of ammonia on iron.[54,55] The study of gas-metal interaction processes by this method is illustrated by the results of a study of the niobium-oxygen system.[32] The catalyst on which the ammonia decomposition and synthesis processes were studied was a strip made of pure iron (99,99% Fe). The ammonia decomposition reaction was studied at an ammonia pressure of

---

*Hereinafter we shall call this layer the surface layer of the solid.

†For brevity, we shall hereinafter call the new method of studying surface processes described in this article the secondary ion emission method. This nomenclature is imprecise, since the method in question includes not only studying the mass spectrum of the secondary ion emission, but also studying the mass spectrum of the ions obtained by ionizing the gas phase.

1×10^{-4} mm Hg in the temperature range from room temperature to 800°C. First of all, the conditions were determined under which the ammonia decomposition reaction takes place. As in [30], the course of the reaction was observed by studying the dependence on the catalyst temperature of the intensities of the lines of the NH_3^+, H_2^+, and N_2^+ ions in the mass spectrum obtained by ionizing the ammonia by electron bombardment. It turned out that the ammonia decomposition reaction does not take place on the surface of the iron strip without prior treatment.

The mass spectrum of the secondary ions sputtered from the surface of such a strip showed a large number of peaks involving the presence of oxygen and iron oxides on the surface. In particular, ions were observed with masses of $16(O^+)$, $32(O_2^+)$, $56(Fe^+)$, $72(FeO^+)$, $88(FeO_2^+)$, $112(Fe_2^+)$, $128(Fe_2O^+)$, $144(Fe_2O_2^+)$, $160(Fe_2O_3^+)$, $176(Fe_2O_4^+)$, $200(Fe_3O_2^+)$, $216(Fe_3O_3^+)$, and $232(Fe_3O_4^+)$. Figure 12 shows the $I(T)$ curves for some of these ions. We see from these curves that oxides on the surface of the iron are observed over the entire temperature range from 20 to 800°C. The hypothesis was advanced that the inactivity of the iron strip with respect to the ammonia decomposition reaction involved the presence of iron oxides on its surface. To test this hypothesis, the iron strip was heated to 800°C for four hours in hydrogen at a pressure of several mm Hg. Then the hydrogen pressure was dropped to 1×10^{-4} mm Hg, and at this hydrogen pressure the relation of the in-
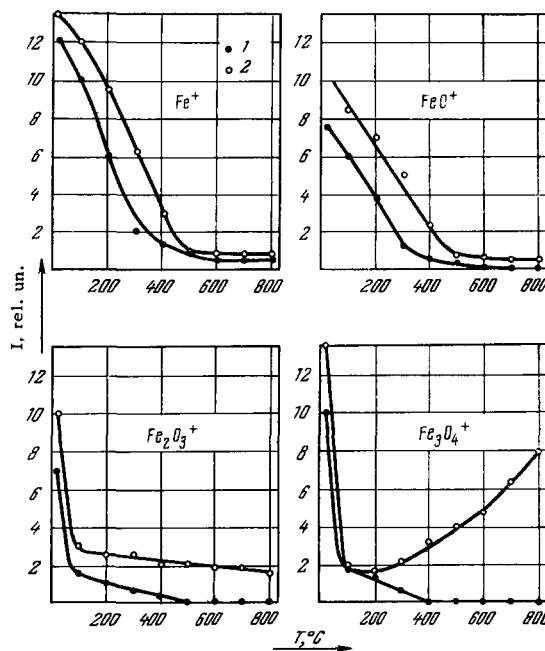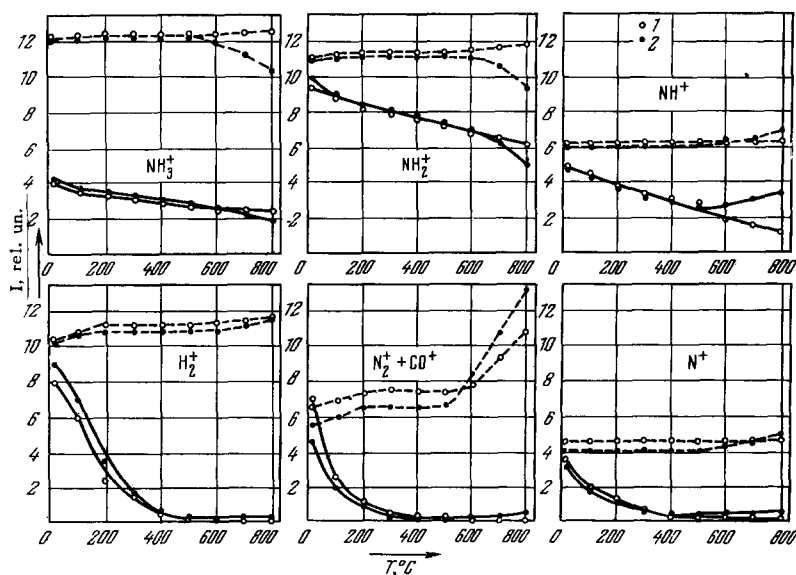

FIG. 12. The relation of the line intensities of the secondary ions Fe^+, FeO^+, $Fe_2O_3^+$, and $Fe_3O_4^+$ to the catalyst temperature when in a hydrogen atmosphere. 1 — active catalyst; 2 — inactive catalyst.

FIG. 13. Relation of the line intensities of the ions NH_3^+, NH_2^+, NH^+, H_2^+, $N_2^+ + CO^+$, and N^+ to the catalyst temperature. Solid curves: secondary ions. Dotted curves: ions obtained by ionizing the gas with an electron beam. 1 — inactive catalyst, and 2 — active catalyst in a hydrogen-ammonia mixture.

tensities of the peaks of the secondary ions Fe^+, FeO^+, $Fe_2O_3^+$, and $Fe_3O_4^+$ to the temperature of the iron strip was again studied. As we see from Fig. 12, which gives the corresponding $I(T)$ curves, the hydrogen treatment considerably decreased the covering of the strip with iron oxides, so that at temperatures above 500°C, iron oxides couldn't be found on the surface of the strip at the maximum sensitivity of the secondary ion detector. The iron strip treated with hydrogen and then kept in a hydrogen atmosphere at 10^{-4} mm Hg pressure proved to be active with regard to the ammonia decomposition reaction. In fact, when ammonia was added to the hydrogen to give a pressure of the ammonia-hydrogen mixture of 2×10^{-4} mm Hg, one could observe the ammonia decomposition reaction on the iron strip, as seen from the $I(T)$ curves for the ions NH_3^+, $N_2^+ + CO^+$, and H_2^+ obtained by ionizing the gas phase by electron bombardment (Fig. 13). As we see from this diagram, the equilibrium pressure of ammonia* in the catalyst chamber begins to diminish at 500°C, and the nitrogen and hydrogen pressures increase. The increase in the amount of ions of mass 28 observed for an inactive catalyst at temperatures above 600°C involves desorption from its surface of CO molecules formed by oxidation of hydrocarbons contained in the residual gas (see[30]). The form of the $I(T)$ curve for these ions does not change after admission of ammonia to the catalyst chamber is stopped. As we see from Fig. 13, the amount of the ions of mass 28 in an ammonia atmosphere in the temperature range above 600°C increases more rapidly with temperature for the active than for the inactive catalyst. The increase

in the equilibrium pressure of hydrogen is weakly marked on the background of the relatively high pressure of hydrogen ($\sim 10^{-4}$ mm Hg), continuously entering the catalyst chamber. Shutting off the hydrogen to the catalyst chamber inactivated the catalyst and stopped the ammonia decomposition reaction. The activity of the catalyst was easily restored by treatment in hydrogen, and was maintained indefinitely as long as an H_2 atmosphere was kept in the catalyst chamber.

Thus there is every ground for stating that the condition for occurrence of the ammonia decomposition reaction is the cleaning of iron oxides from the catalyst surface. The presence of a hydrogen atmosphere hinders formation of oxides on the catalyst surface at temperatures above 500°C, and this makes possible the ammonia decomposition reaction at these temperatures.

Figure 13 shows the $I(T)$ curves for the ions NH_3^+, NH_2^+, NH^+, $N_2^+ + CO^+$, H_2^+, and N^+, both when sputtered from the catalyst surface and when obtained by ionizing the gas phase by electron bombardment. We see from this diagram that the shape of the $I(T)$ curves differs substantially for the active and the inactive catalyst. Comparison and analysis of these curves permits us to hypothesize on the most probable nature of the elementary processes in the catalytic decomposition of ammonia on iron.

Just as with a platinum catalyst,[30] the first stage in the process of decomposition of ammonia at temperatures above 500°C is the decomposition of part of the NH_3 molecules adsorbed on the surface of the iron, according to the equation $NH_3 \rightarrow NH + H_2$, with subsequent desorption of NH and H_2 into the gas phase.

Formation of NH particles by dissociative adsorption of NH_3 has been firmly established on the basis of the following facts.

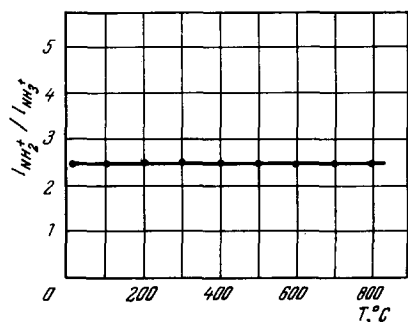*The measurements were made in a dynamic system with continuous admission of ammonia into the catalyst chamber and continuous pumping of ammonia and its decomposition products from the chamber.

FIG. 14. The $I_{NH_2^+}/I_{NH_3^+}$ ratio as a function of the temperature.

1) The emission of NH^+ secondary ions increases over the temperature range 500—800°C, while the emission of NH_3^+ and NH_2^+ ions declines. This difference in the trend of the $I(T)$ curves for the NH^+ and NH_3^+ ions in the stated temperature range indicates that the NH^+ ions arise not only as fragments of NH_3 particles upon primary-ion impact, but they are also ejected from NH particles formed by the decomposition of ammonia.

The temperature-independence of the ratio $I_{NH_2^+}/I_{NH_3^+}$ (Fig. 14) indicates that NH_2 particles are not formed in appreciable amount in the decomposition of ammonia, whereas the NH_2^+ ions are fragments of NH_3 molecules (see below).

2) Over the same temperature range, the intensity of the NH^+ ion beam obtained by electron-bombardment ionization increases, in spite of the decrease in the amount of NH_3 molecules in the gas phase. This fact is explained by desorption of NH particles into the gas phase.

Thus, the NH molecules formed in the first stage of the ammonia-decomposition process are partly desorbed into the gas phase. Another fraction of these molecules reacts on the catalyst surface according to the equation $NH + NH \rightarrow N_2 + H_2$. The N_2 and H_2 molecules formed in this stage of the process are desorbed into the gas phase. The mechanism for the catalytic decomposition of ammonia on iron proposed on the basis of the experimental results obtained in this study agrees completely with the mechanism of decomposition of ammonia previously established for a platinum catalyst.[30] Apparently this agreement is not fortuitous, and might serve as an argument favoring the hypothesis advanced in[56] that the mechanisms of decomposition of ammonia are the same for a number of catalysts.

We should note in conclusion that the mass spectrum of the secondary ions sputtered from an iron surface in an ammonia atmosphere contained FeN^+ ions. The emission of these ions involves formation of iron nitride on the surface of the catalyst. Emission of FeN^+ secondary ions monotonically declined with increasing catalyst temperature, and could no longer be detected above 500°C at the maximum sensi-

tivity of the secondary-ion detector. This implies that iron nitride exists on the catalyst surface in appreciable quantities below 500°C. We shall now proceed to present the results of the study of ammonia synthesis on the same iron catalyst on which the ammonia decomposition reaction was studied.

We should point out a peculiarity of the ammonia synthesis reaction, as compared with other reactions that have been studied by the secondary ion emission method. As with every mass-spectrometric method, this method is suitable for studying catalytic reactions only at low pressures of the mixture of reacting gases (of the order of 10^{-4} mm Hg). However, as shown by calculation, when the pressure of the nitrogen-hydrogen mixture is 10^{-4} mm Hg, the equilibrium ammonia pressure is 1.7×10^{-14} mm Hg. Evidently, at such a low ammonia pressure we can get no information on the course of the catalytic reaction by observing the mass spectrum from electron-impact ionization of the gas phase, as was done in the studies on ammonia decomposition. In this case all conclusions on the reaction mechanism had to be made only from study of the mass spectrum of the secondary ion-ion emission.

The synthesis reaction was studied at a pressure of the nitrogen-hydrogen mixture of 1.2×10^{-4} mm Hg. The $N_2 : H_2$ partial pressure ratio was 1:3 (stoichiometric mixture). The reaction was studied over the temperature range 20—800°C.

As was stated above, an untreated iron strip is inactive with respect to the ammonia decomposition reaction. Only after heating in hydrogen does the iron strip become active with respect to this reaction, and this activity is maintained while the strip is kept in a hydrogen atmosphere. As we should expect, iron that was active for the ammonia decomposition reaction proved also to be active for the ammonia synthesis reaction. The activity of the catalyst with respect to the ammonia synthesis reaction could be determined from the $I(T)$ relation for NH_3^+ ions. As we see
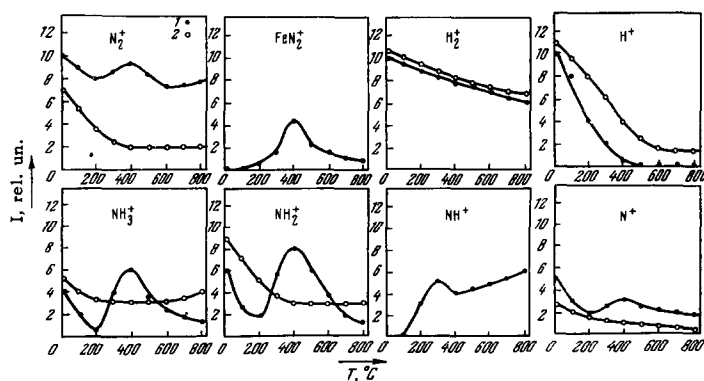

FIG. 15. The I(T) curves (in relative units) for secondary ions (for an active (1) and an inactive (2) catalyst) in a nitrogen-hydrogen mixture having $p_{N_2} = 3 \times 10^{-5}$ mm Hg and $p_{H_2} = 9 \times 10^{-5}$ mm Hg.

from Fig. 15, the presence of NH_3 molecules* on the catalyst surface becomes appreciable at ~ 200°C. When the catalyst temperature is raised further, the covering of its surface by NH_3 molecules reaches a maximum at ~400°C, and then declines monotonically. The process of ammonia synthesis was also studied in a $D_2 + N_2^{15}$ mixture. In this case, the formation of ammonia on the catalyst surface was indicated by the appearance of ions of mass 21($N^{15}D_3^+$). The $N^{15}D_3^+$ ions appeared at ~ 150°C. The shape of the I(T) curve for the $N^{15}D_3^+$ ions was quite similar to that for NH_3^+ ions.

In order to determine the nature of the elementary processes occurring on the catalyst surface, I(T) curves were obtained for the ions NH_3^+, NH_2^+, and NH^+ characterizing the NH_3 molecule and its fragments formed by interaction with a primary ion, and for the ions H_2^+, H^+, N_2^+, and N^+ characterizing the molecules of the reacting gases and their fragments. In addition, it was found that FeN_2^+ ions are sputtered from the from the catalyst surface while the ammonia synthesis reaction is occurring on it. The I(T) curve was also determined for these ions.

It was of interest to determine which of two mechanisms the ammonia synthesis reaction followed, the Langmuir–Hinshelwood mechanism (the reacting particles enter into reaction on the catalyst surface), or the Rideal mechanism (one of the reacting particles is adsorbed on the surface of the catalyst, but the other one reacting with it comes from the gas phase). For this purpose, curves were obtained for the relation of the intensity of the NH_3^+ ion beam to the hydrogen and nitrogen pressures. The same curves were obtained for the FeN_2^+ ion.

Figures 15 and 16 show the I(T) and I(p) curves, respectively, for the ions cited above.

Just as in the case of separate adsorption of nitrogen and hydrogen,[55] and observe no dissociation of N_2 and H_2 molecules into atoms under the conditions of the ammonia synthesis reaction on iron. This conclusion follows from examining the I(T) curves for the N_2^+, N^+, H_2^+, and H^+ ions in Fig. 15. One can conclude from the shape of the I(T) curve for N_2^+ ions that these ions are sputtered both from adsorbed N_2 molecules and from molecules of the nitride FeN_2. The increase in the N_2^+ ion beam intensity at temperatures above 600°C involves an increase in the cover-

ing of the catalyst surface with N_2 molecules formed in the ammonia decomposition reaction.

It is a very important fact that the shape of the I(T) curves for the NH_3^+ and FeN_2^+ ions is identical. The similarity of shape of the I(T) curves for these ions can be explained in two ways: 1) NH_3 molecules produced on the surface of the catalyst react with it to form molecules of the iron nitride FeN_2, and 2) nitrogen chemisorbed on the catalyst surface forms FeN_2, and then hydrogenation of the chemisorbed nitrogen gives rise to NH_3 molecules. We must reject the first of these explanations on the basis of the results of the ammonia decomposition study. First, they show that the iron nitride FeN is formed when ammonia acts on the surface of the active catalyst. Second, the number of FeN molecules on the catalyst surface becomes vanishingly small at temperatures above 500°C. Thus there remains only the second possibility of explaining the formation of FeN_2 on the surface of the catalyst. That is, formation of the iron nitride FeN_2 proves to be the first stage in the ammonia synthesis reaction.

As for the second stage in the ammonia synthesis reaction, we can draw a definite conclusion by comparing the I(T) curves for the ions NH_3^+, NH_2^+, and NH^+. The $I_{NH_2^+}/I_{NH_3^+}$ ratio is independent of the catalyst temperature over the range 20–800°C. Thus we can conclude that the ion NH_2^+ is a fragment of the NH_3 molecule formed by dissociative ionization of this molecule by primary-ion impact.

The $I_{NH^+}/I_{NH_3^+}$ ratio varies with varying catalyst temperature over the entire range 20–800°C. This means that the NH^+ ion is ejected not only from NH_3 molecules, but also from some other particle. This particle could only be the NH radical. As was shown above, this radical is formed on the surface in the ammonia decomposition reaction. However, it has

---

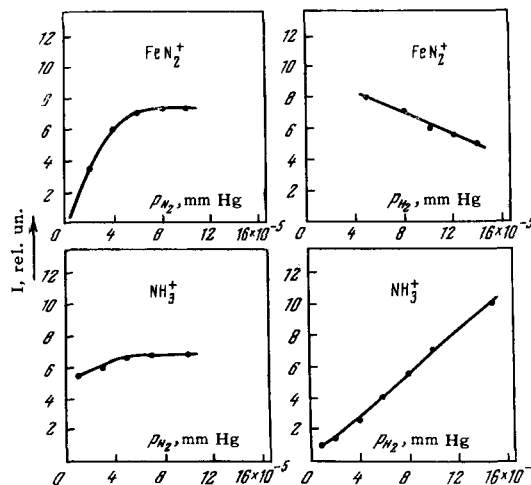*The emission of secondary ions of mass 17 (OH^+ ions) at temperatures below 200°C involves existence on the catalyst surface of adsorbed H_2O molecules. The decrease in the intensity of the OH^+ ion beam over the temperature range $20 < T < 200$°C involves desorption of H_2O molecules from the surface of the active catalyst. We can understand the course of the I(T) curve for OH^+ ions for the inactive catalyst if we bear in mind the fact that oxides on the iron surface are reduced in the hydrogen atmosphere, and this is accompanied by the appearance of H_2O molecules on its surface.

FIG. 16. The I(p) curves (in relative units) for the secondary ions NH_3^+ and FeN_2^+ at 400°C.

been established [54] that the ammonia decomposition reaction proceeds at an appreciable rate at temperatures above 500°C. Thus, at temperatures below 500°C the NH particle must be formed on the catalyst surface by another process. This process is the hydrogenation of the surface nitride FeN_2. That is, the NH particle is produced by the reaction $FeN_2 + H_2 \rightarrow Fe{\Large\diagdown}^{NH}_{NH}$. From this standpoint, the shape of the I(T) curve for NH^+ ions is explained as follows. In the temperature range 100–400°C, Fe—NH complexes and NH_3 molecules on the catalyst surface play the determining role in fixing the course of this curve. In this temperature range, the NH^+ ions are ejected only from these particles. At temperatures above 400°C, NH particles appear on the catalyst surface, owing to the fact that the rate of the ammonia decomposition reaction becomes appreciable. The rate of the ammonia decomposition reaction increases with rising temperature (see Fig. 13). This is the reason for the rising branch on the I(T) curve for NH^+ ions in the temperature range above 500°C.
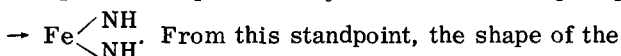
Evidently, the third stage of the ammonia synthesis reaction is the hydrogenation of the NH radical according to the equation Fe—NH + $H_2 \rightarrow$ Fe—NH_3. The NH_3 molecule formed can then be desorbed into the gas phase. Thus, on the basis of the set of I(T) curves in Fig. 15, we can conclude that the ammonia synthesis reaction on iron consists of the following stages:

I. $\quad\quad\quad\quad$ Fe $+$ N$_2 \rightarrow$ FeN$_2$,

II. $\quad\quad$ FeN$_2 +$ H$_2 \rightarrow$ Fe${\Large\diagdown}^{NH}_{NH}$,

III. $\quad\quad$ Fe $-$ NH $+$ H$_2 \rightarrow$ Fe $-$ NH$_3$.
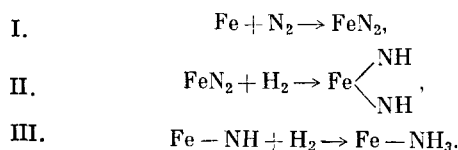
Examination of the I(p) curves in Fig. 16 also makes possible some conclusions. As we see from this diagram, the covering of the catalyst by molecules of the nitride FeN_2 attains saturation with increasing nitrogen pressure. An analogous situation occurs also in the variation of the covering of the catalyst surface by NH_3 molecules. However, the yield of ammonia increases linearly with increasing hydrogen pressure. We can draw from these data the conclusion that the ammonia synthesis mechanism on iron follows the Rideal mechanism. The reaction occurs between N_2 molecules chemisorbed on the catalyst surface and hydrogen molecules arriving from the gas phase. One can understand why the covering of the catalyst by chemisorbed nitrogen decreases with increasing hydrogen pressure (the I(p_{H_2}) curve for FeN$_2^+$ ions in Fig. 16). This is because a fraction of the chemisorbed nitrogen molecules are transformed into ammonia molecules as the hydrogen pressure increases. Thus we should expect that the I(p_{H_2}) curve for NH$_3^+$ ions at higher pressures should show a decline in the rate of increase in the number of NH_3 molecules with increasing hydrogen pressure. This means that, in order to increase the yield of ammonia, one must not only increase the hydrogen pressure but also the nitrogen pressure.

In view of the great industrial importance of the ammonia synthesis reaction, the kinetics of this reaction has been studied in detail. Owing to the low yield of ammonia at low pressures of the nitrogen-hydrogen mixture, the kinetics of ammonia synthesis has been studied at atmospheric and higher pressures. A doubly-promoted catalyst of the industrial type has been used as the catalyst in most cases.

The data existing in the literature on the mechanism of ammonia synthesis have been based on the kinetic measurements mentioned above, together with studies of the adsorption of nitrogen, hydrogen, and ammonia. Based on these indirect data, there exist at present two basic conceptions on the mechanism of ammonia synthesis. One of these is held by Horiuti and his school, [57] and consists in the idea that nitrogen and hydrogen adsorbed on the catalyst surface dissociate into atoms. Ammonia synthesis occurs in several stages by association of one nitrogen atom and three hydrogen atoms.

M. I. Temkin and his school [58-60] have proposed another idea based on many years of studies. According to this view, the first stage of the ammonia synthesis reaction is the chemisorption of molecular nitrogen. In the second stage, the chemisorbed nitrogen is hydrogenated to form the adsorbed radical NH. Finally, an NH_3 molecule is formed by a second hydrogenation of this radical (the third stage), and is then desorbed into the gas phase.

The results of the present study totally contradict the views of Horiuti's school on the mechanism of ammonia synthesis. The process of the synthesis reaction did not manifest formation of H or N atoms or NH_2 radicals, which must exist on the surface of the catalyst if the synthesis reaction passes through the stages proposed by Horiuti.*

On the other hand, the system of elementary processes in the ammonia synthesis reaction established in our work completely agrees with the analogous system proposed by M. I. Temkin and his associates. We can draw from this agreement the very important conclusion that the mechanism of the ammonia synthesis reaction does not depend on the pressure of the mixture of reacting gases over the pressure range from 10^{-4} mm Hg to one atmosphere. Apparently, this conclusion can be extended even to pressures of the order of hundreds of atmospheres, since the Temkin-Pyzhev kinetic equation is valid even at these pressures.

---

*The error in Horiuti's view of the mechanism of ammonia synthesis has also been established in a paper given by Tanaka at the 3rd International Congress on Catalysis (see the report on this congress by G. K. Boreskov [61]).

The conclusion that the mechanism of the catalytic reaction is independent of the pressure of the mixture of reacting gases above the catalyst surface is also implied by general considerations. In fact, catalytic processes occur in the film of gases adsorbed on the catalyst surface. The concentration of matter in this film is very large, and corresponds to gas pressures of the order of thousands of atmospheres. Naturally, an increase of the pressure of the mixture of reacting gases, even to hundreds of atmospheres, cannot affect the nature of the elementary processes on the catalyst surface as established at low pressures. This circumstance strongly enhances the value of the secondary ion-ion emission method, since it becomes possible to ascribe a mechanism of a catalytic reaction determined by this method at pressures of the order of 10^{-4} mm Hg to the same reaction occurring under industrial conditions at high pressures.

As for the nature of the information that the secondary ion emission method can provide in studying gaseous corrosion, we can gain an idea from the results presented below from a study of the reaction of oxygen with niobium.[32]

Corrosion processes differ substantially from catalytic processes in that they do not occur in a monomolecular film, as do the latter. Rather, they begin at the surface of the metal, and then, owing to diffusion of the reacting particles, they propagate into the interior of the metal. This leads to formation of a tarnish film of considerable thickness. The structure and chemical composition of tarnish films on the surface of metals have been successfully studied by a number of methods. On the other hand, the existing methods of studying corrosion do not permit study of the initial stage of the corrosion process, i.e., the stage of formation of surface chemical compounds.* The secondary ions of the chemical compounds of the metal with molecules of the surrounding gaseous medium observed in the secondary ion emission spectrum most probably arise from interaction of primary ions with the superficial (possibly monomolecular) film on the surface of the metal. It is precisely because of this situation that the study of the relation of the beam intensities of these secondary ions to the temperature of the metal and the nature and pressure of the gaseous medium permits one to get information on the initial stage of corrosion processes. This is confirmed by the results presented below from the study of the niobium-oxygen system.

A niobium strip was put into the target chamber, and at first was heated in vacuo to 2000°C for ten minutes. Then, after it had cooled to room temperature, the mass spectrum of the ions sputtered from its surface was studied. In addition to positive and negative ions involving the presence on the surface of the niobium of adsorbed molecules of the residual gases, the secondary-ion mass spectrum also showed ions involving the presence of oxides on the surface (Nb^+, $NbO^{\pm}$, $NbO_2^{\pm}$, Nb_2O^+, $Nb_2O_2^+$, $Nb_2O_3^{\pm}$, $Nb_2O_4^+$, $Nb_2O_5^+$).

Heating the niobium strip in the atmosphere of residual gases to 2000°C leads to disappearance of the emission of all secondary ions but that of Nb^+ ions. The intensity of the Nb^+ ion beam at 2000°C is two orders of magnitude smaller than that at room temperature. The disappearance of the secondary ion emission permits us to state that the Nb surface heated to 2000°C in the residual gas at a pressure of 5×10^{-6} mm Hg is cleaned of adsorbed particles and oxides. Independently of the temperature in the range 1500–2000°C, the emission of secondary Nb^+ ions involves the sputtering of these ions from the crystal structure of the metal. After the specimen had been cooled to room temperature, the emission of all the secondary ions was completely restored.

Some conclusions on the composition of the oxides on the Nb surface in the residual-gas atmosphere and in oxygen at a pressure of 5×10^{-5} mm Hg at various temperatures of the niobium strip can be drawn from examining Fig. 5. This diagram shows the $I(T)$ curves for the ions involving oxides on the niobium surface. These curves were obtained as follows. At first, the niobium strip was heated to 2000°C and thus its surface was cleaned of adsorbed particles and oxides. Then, the temperature was lowered to room temperature in stages. At a number of points in the temperature range 20–2000°C, measurements were made of the beam intensities of the secondary ions being studied. That is, the $I(T)$ curves were obtained for decreasing temperature of the niobium strip. After room temperature had been reached, the temperature of the niobium was raised, and $I(T)$ curves were again taken up to 2000°C. It turned out that the $I(T)$ curves obtained on lowering the niobium temperature from 2000°C agreed with those then obtained on raising the temperature from 20 to 2000°C within the limits of experimental error. Similar situations occurred both in the residual-gas atmosphere and in the oxygen atmosphere at 5×10^{-5} mm Hg. The cited facts imply that, under the described experimental conditions, an initially clean Nb surface passes through a series of states upon cooling, which are then reproduced upon subsequent heating.*

---

*The possibility is not excluded of applying the infrared adsorption method to study gaseous corrosion. However, in view of the specific difficulties of preparing specimens to study surface processes by this method, it can hardly become of universal importance in studying the initial stage of corrosion processes.

*Visual observation of the niobium strip, when taken from the chamber after this experiment had been performed, showed that it had kept its metallic luster. A microphotograph of the surface of the strip showed no patches of oxides.

Examination of the I(T) curves in Fig. 5 permits us to draw some conclusions. The shape of the I(T) curves for the pairs of ions NbO^+ and Nb^+, $Nb_2O_3^+$ and Nb_2O^+, and $Nb_2O_5^+$ and $Nb_2O_4^+$ is identical. On the other hand, each pair of cited ions has its own characteristic form of I(T) curve differing from those for the other pairs. Hence we can conclude that the ions NbO^+ and Nb^+ are sputtered from the oxide NbO, the ions $Nb_2O_3^+$ and Nb_2O^+ from the oxide Nb_2O_3, and the ions $Nb_2O_5^+$ and $Nb_2O_4^+$ from the oxide Nb_2O_5. The shape of the I(T) curve for the NbO_2^+ ion differs from that of all the other I(T) curves. Hence we can conclude that the NbO_2^+ ions are sputtered from the oxide NbO_2. Thus by analyzing the I(T) curves given in Fig. 5 we can conclude that over a certain temperature range (20–2000°C at an oxygen pressure of 5×10^{-5} mm Hg), the oxides NbO, Nb_2O_3, NbO_2, and Nb_2O_5 exist on the Nb surface.*

The relative concentration of these oxides on the Nb surface depends on the temperature of its surface and the oxygen pressure. The effect of the oxygen pressure on the concentration of any particular oxide on the surface of the niobium is illustrated by the I(T) curves for the ion $Nb_2O_3^+$ obtained at different oxygen pressures (see Fig. 5). As we see from this diagram, the peak of the I(T) curve is shifted to higher temperatures with increasing oxygen pressure.

The mass spectrum from ionization of the gas phase showed only NbO^+ ions. The existence of these ions in the mass spectrum indicated the desorption of the oxide NbO from the Nb surface. As we see from Fig. 17b (dotted curve), this desorption begins to be observed at 1400°C, and the rate of desorption swiftly increases with further rise in temperature. Along with desorption of the NbO molecule in the neutral state, desorption of NbO^+ and Nb^+ ions was also observed (solid curves in Fig. 17b).† The thermoemission flux of NbO^+ and Nb^+ ions increases with increasing oxygen pressure (the $I(p_{O_2})$ curves for the thermoions NbO^+ and Nb^+ in Fig. 17a). Desorption of NbO molecules and NbO^+ ions is not observed in a residual-gas atmosphere at 2000°C, and correspondingly, emission of secondary NbO^+ ions is also not observed. The oxide NbO is formed on the Nb surface with increasing partial pressure of oxygen, as indicated by appearance of emission of secondary NbO^+ ions and desorption of NbO molecules and NbO^+ ions into the gas phase. The data of the experiment, as illustrated by the I(T) and $I(p_{O_2})$ curves of Fig. 17, show that at high Nb temperatures

---

*The shape of the I(T) curves for the ions NbO^-, NbO_2^-, and $Nb_2O_5^-$ is the same as that of the corresponding curves for the ions $Nb_2O_3^+$ and $Nb_2O_4^+$. Apparently, these ions are also sputtered from the surface oxide Nb_2O_5.

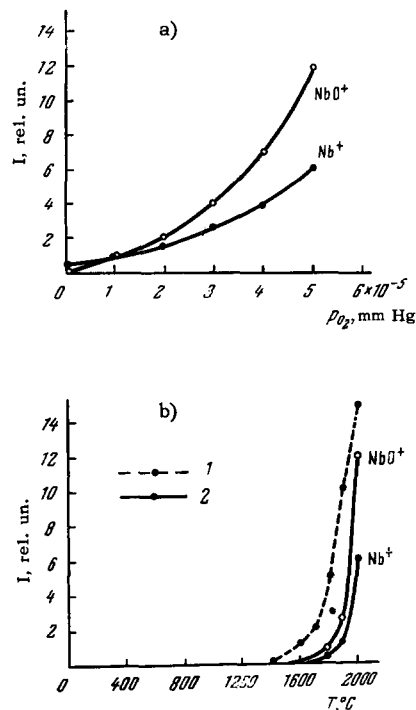†Thermoemission of Nb^+ and NbO^+ ions from a heated niobium surface has also been observed in [62].

FIG. 17. a) The $I(p_{O_2})$ functions at T = 2000°C for the thermoemission ions Nb^+ and NbO^+. b) The function I(T) for the ions Nb^+ and NbO^+ at $p_{O_2} = 5 \times 10^{-5}$ mm Hg. 1 – NbO^+ ions from ionization of the gas phase; 2 – thermoions.

and low oxygen pressures, the corrosive loss of Nb occurs by formation of the oxide NbO on its surface and subsequent vaporization into the gas phase.

Some interesting phenomena occurring in the interaction of oxygen with a heated Nb surface are illustrated by the curves in Fig. 18. This diagram shows the I(T) curves for the O_2^+ and O^+ ions, both as
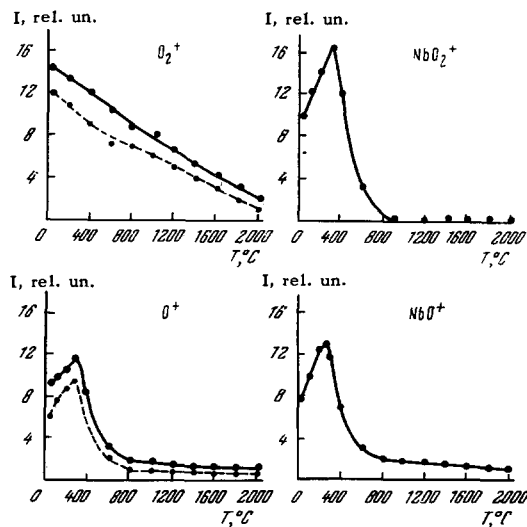

FIG. 18. The I(T) functions for the ions O^+, O_2^+, NbO^+, and NbO_2^+. Solid curves for secondary ions. Dotted curves for ions from ionizing the gas phase.

secondary ions and as obtained by ionizing the gas phase. For comparison, this same diagram also shows the $I(T)$ curves for the secondary ions NbO_2^+ and NbO^+. Comparison of the $I(T)$ curves for the O_2^+ and O^+ ions permits us to conclude that the process of transformation of molecular into atomic oxygen occurs on the Nb surface over the temperature range from $20°$ to about $800°C$, with subsequent desorption of atomic oxygen into the gas phase. This transformation could hardly be a catalytic dissociation of oxygen on the Nb surface, since under this assumption it would still not be understandable why this process has a maximum at $300°C$. On the other hand, attention is drawn to the close similarity in shape of the $I(T)$ curves for the O^+, NbO_2^+, and NbO^+ ions. On the basis of this fact, we can advance a hypothesis explaining the phenomenon of transformation of molecular into atomic oxygen on a Nb surface. This hypothesis consists in the following. A molecule of O_2 reacts with the Nb surface to form the oxide NbO_2. This oxide partially decomposes according to to the equation $NbO_2 \rightarrow NbO + 0$, and the atomic oxygen formed is desorbed into the gas phase. Thus, the transformation of molecular into atomic oxygen is a result of the oxidation reaction of Nb, with subsequent decomposition of the oxide formed. The experiments described above show that use of the secondary ion emission method makes it possible to study the initial stage of the oxidation of niobium. This method has also been applied to study the reaction of oxygen with silver[28] and iron.[31]

In closing this section of the article, we shall discuss some critical remarks that might be made on the application of the secondary ion emission method to study surface processes.

One of these remarks involves the shape of the $I(T)$ curves. The number N_i of secondary ions is related to the surface concentration N of particles, from which they are sputtered according to the relation

$$N_i = \alpha_i N, \qquad (4)$$

where α_i is the sputtering probability of the ions. The interpretation of results obtained by the secondary ion emission method is based on the assumption that the temperature-dependence of N_i is related to the temperature-dependence of the surface concentration N. It is assumed that α_i does not depend on the temperature. If this quantity were substantially temperature-dependent, this would greatly complicate the interpretation of the results obtained by the secondary ion emission method.

The question arises of how valid the assumption is that the probability of ion sputtering is temperature-independent. This question could be answered directly by an experiment simultaneously measuring both the number of sputtered secondary ions and the surface concentration of particles from which they were

sputtered. An experiment of this type is rather difficult, and has not yet been performed. However, there are many experimental data indirectly confirming the assumption that the probability of sputtering of secondary ions is independent of (or weakly dependent on) the temperature. The case in which constant N is realized for the surface of a metal cleaned of adsorbed particles and surface compounds. This situation exists for Nb in a residual-gas atmosphere over the temperature range $1500-2000°C$ (see Fig. 5). As we see from this diagram, the intensity of the Nb^+ ion beam is constant over this temperature range. This indicates that their sputtering probability is constant. Below $1500°C$, the oxide NbO appears on the surface of the niobium and Nb^+ ions are also sputtered from it. Then the intensity of the Nb^+ ion beam begins to vary with the temperature in correspondence with the coverage of the niobium surface with the oxide NbO. This can be seen by comparing the $I(T)$ curves for the ions Nb^+ and NbO^+. An example of this type is also given by the $I(T)$ curve for Mo^+ ions.[21,23] After a molybdenum surface has been cleaned of oxides, the Mo^+ ion beam intensity ceases to vary with further increase in temperature.

If the sputtering probability of secondary ions were temperature-dependent, this dependence would be monotonic in nature. However, there are many cases in which the $I(T)$ curves have non-monotonic courses. This can be explained only by corresponding variations in the surface concentrations of molecules of adsorbed gases and of surface compounds. Such, for example, are the $I(T)$ curves for H_2O^+ ions in the oxidation of ammonia on platinum,[51] for C_2^- ions for an unactivated catalyst in the decomposition of ammonia[30] (see Fig. 3), and for H_2O^+ ions in the NO + NH_3 reaction,[53] etc. On the other hand, one observes in many cases a monotonic decline in the secondary-ion beam intensity with increasing target temperature. This involves the desorption into the gas phase of the particles responsible for the secondary ion emission. These facts permit us to state that temperature-dependence of the probability of secondary-ion sputtering can hardly affect the conclusions drawn from the shape of the $I(T)$ curves.

As was stated above, when a primary ion interacts with a molecule on the surface of a metal, not only the secondary ions corresponding to the unfragmented molecule are sputtered, but also fragmentary ions involving dissociation of the molecule by the impact of the primary ion. The question arises of how much the dissociation of the molecules by primary-ion impact can affect the interpretation of the results obtained by the secondary ion emission method. In particular, can one unequivocally establish the origin of the fragmentary ions, bearing in mind the fact that dissociation of adsorbed molecules can also stem from adsorptive forces, and that these ions can be sputtered from a fragment of the molecule that had been disso-

ciated upon adsorption? A criterion is pointed out
in [51] by which one can determine whether a given
secondary ion is a fragment of a more complex mole-
cule, or whether its presence in the mass spectrum
involves the existence on the solid surface of a mole-
cule identical to it in composition.

Finally, we should discuss the problem of the pos-
sible influence of the bombardment of the target by
the primary-ion beam on the course of the processes
on its surface.

The effect of the primary beam on the processes
being studied can be diminished by establishing the
following experimental conditions:

a) Choice of primary-beam particles that are
chemically inert and weakly adsorbed by the metal
surface.

b) Decrease in the current density of the bombard-
ing ions.

c) Decrease in the velocity of the bombarding ions.

d) Decrease in the time of action of the bombarding
ions on the surface, i.e., making the measurements
with the primary beam current applied in short pulses.

We might state that the conditions under which the
secondary ion emission method has been applied to
study surface processes (Ar^+ ions of velocity
3.2×10^7 cm/sec, current density 10^{-8} A/mm^2, con-
tinuous operation) have not affected the course of
these processes. For example, this statement is
based on the fact that the I(T) curves for the second-
ary and the gaseous NO$^+$ ions are identical in the ox-
idation of ammonia on platinum (see Fig. 1 in [51]). It
is easy to see that the temperature-dependence of the
rate of oxidation of ammonia for the region of the
catalyst surface being bombarded by the ion beam is
described by the I(T) curve for the secondary NO$^+$
ions. The I(T) curve for the gaseous NO$^+$ ions gives
the dependence of the reaction rate on the catalyst
temperature for all the rest of the surface of the
catalyst, which had an area about fifty times as great
as the area of the catalyst bombarded by the ion beam.
Similar situations occurred also in other studied re-
actions, e.g., in the formation of N$_2$ in the catalytic
reaction between nitric oxide and ammonia.[53]

Summing up all that has been said in this section
of the article, we can state that the new method of
studying surface processes, which is based on using
the phenomenon of secondary ion emission, provides
new and valuable information. Hence, its further de-
velopment and refinement are expedient with regard
to its subsequent application to a wide range of ad-
sorption, catalytic, and corrosion processes.

b) An ion microscope based on the phenomenon of secondary ion emission

Secondary ions sputtered from a solid surface by
a primary beam can be focused by a system of elec-
trostatic lenses as used in electron microscopes, and
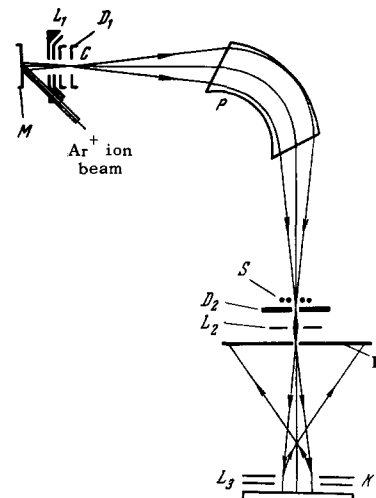a magnified image of the target surface can be ob-

FIG. 19.

tained on a screen. The image obtained will be formed
by all the secondary ions. However, if the secondary-
ion beam focused by the electrostatic lenses is passed
through a magnetic prism, then one can get an image
of the target surface on the screen that is formed by
ions of a definite mass. The value of the mass of the
ion used to form the image is determined by the field
intensity of the magnetic prism. By changing the
direction of the electric and magnetic fields one can
obtain an image both with positive and with negative
ions.

This idea has been applied in an ion microscope
based on the phenomenon of secondary ion emission.
It has been built in France in the Institut National
des Sciences Appliquées [63] and in the Department of
Solid State Physics of the University of Paris.[64,65]
The ion microscope built at the University of Paris
will be described below.

Figure 19 shows the basic diagram of the ion
microscope based on secondary ion emission. A beam
of Ar^+ ions of energy 10 keV falls on the target sur-
face M. The beam of secondary ions sputtered from
the target is accelerated and focused by the electro-
static lens L$_1$. The diaphragm D$_1$ is placed at the
focus C of this lens. The purpose of the diaphragm
is to decrease the scatter in the velocity component
perpendicular to the beam axis in the beam passing
through the diaphragm. The magnetic prism P serves
to isolate a component of definite mass from the beam
of focused secondary ions. The entrance and exit
angles of the beam in the magnetic field are chosen
such that the fringe magnetic field produces focusing
in two directions, in the direction of the magnetic
field and perpendicular to it. Astigmatism of the mag-
netic prism arises from the fact that the focal points
for these two directions do not coincide. It is cor-
rected by applying an additional electric field between
the grid S and the exit slit D$_2$ of the magnetic prism.
The beam of ions of definite mass passing through the

FIG. 20. [Translator's note: The reader is referred to [⁶⁴] for the much clearer originals from which this figure was taken, and which show some interesting features lost in reproduction, e.g., the close similarity of pictures 1 and 3.]

slit D_2 is focused by the electrostatic lens L_2 on the cathode of the ion-electron converter K. The electrostatic lens L_3 produces an image of the target surface on the fluorescent screen E from the electrons ejected from the cathode K. This image can be photographed through a lateral viewing window. The described ion microscope can be easily transformed into a mass spectrometer by placing a Faraday cylinder after the slit D_2 to measure the ion current. This is the instrument on which[26] was done.

The ion microscope based on the phenomenon of secondary ion emission can be successfully used to study inhomogeneous surfaces. To illustrate the possibilities of the ion microscope, the authors of[64] give three photographs of the surface of an Al-Mg-Si alloy (Fig. 20) taken with the ions $^{24}Mg^+$ (1), Al^+ (2), and $^{28}Si^+$ (3). Each of these pictures gives the distribution of the corresponding component of the alloy on the surface of the specimen. The authors of this study point out that one can attain a resolution of the order of 0.03μ with the ion microscope that they have built.

Undoubtedly, the design of the ion microscope discussed above will prove very useful in studying adsorption and catalytic processes on inhomogeneous surfaces. In particular, one very important experiment might be pointed out that could be performed with this ion microscope. One of the theories of catalysis is the so-called active-center theory. The essence of this theory consists in the assumption that not all of the catalyst surface possesses catalytic activity, but only certain regions of it, or active centers. There is no single opinion on the physical nature of the active centers. No direct experimental proof has yet been given for the existence of active centers. By using the ion microscope based on secondary ion emission, one could try to answer the question of the existence of active centers. Using the example of the ammonia synthesis reaction on iron, we can explain how one could perform the experiment in question. FeN_2 molecules are produced on the catalyst surface in the process of ammonia synthesis on iron, as indicated by the appearance of emission of secondary FeN_2^+ ions (see Figs. 15, 16). Quite understandably, the FeN_2 molecules appear on the catalytically active regions of the surface of the iron. If now we take an

iron catalyst as the object of the ion microscope, and take a picture of its surface using FeN_2^+ ions during the process of ammonia synthesis, then this picture will give the distribution over the catalyst surface of the regions showing catalytic activity.

c) Application of secondary ion emission to analyze the composition of solids

The existence of ions of the substance comprising a solid in the composition of the secondary ion emission provides a basis for developing a method of analyzing solids by measuring the beam intensities of these ions.

The first attempt to analyze a Ge-Si alloy from the ratio of the beam intensities of the Ge^+ and Si^+ ions was made in[20]. It turned out that the I_{Si^+}/I_{Ge^+} ratio differs from the Si concentration in the alloy, and depends on the energy of the primary ions. This result is not surprising if we bear in mind that the sputtering coefficients of the Ge^+ and Si^+ ions from a Ge-Si alloy can differ, while their dependences on the primary-ion energy might also not be identical.

Some preliminary studies of the ratio of beam intensities of the secondary ions of the components of Cu-Ni and Cu-Al binary alloys have been made in[26]. It turned out that the sputtering coefficient of Cu^+ ions from a Cu-Al alloy is ten times as great as from a Cu-Ni alloy. The authors of this study also concluded that the quantity I_1/I_2 (the ratio of beam intensities of the secondary ions of the components of the alloy) is not equal to the ratio S_1/S_2 of the concentrations of the alloy components.

The inequality of I_1/I_2 and S_1/S_2 is not a hindrance to developing an analytical method, since one can construct in advance a calibration curve $I_1/I_2 = f(S_1/S_2)$ for a series of alloys of known concentrations of the components. A more serious difficulty is that the ions of the substance of the solid are sputtered not only from its crystal structure, but also from chemical compounds of its atoms with molecules of the surrounding residual gas. In the concrete case of a binary alloy, this means that the ratio I_1/I_2 will depend on the state of its surface, or in other words, on the covering of its surface by molecules of chemical compounds of atoms of the alloy with molecules of the

residual gas. One must make a special study to determine the conditions (target temperature, pressure and composition of the residual gas) under which the quantity I_1/I_2 will be reproducible with sufficient accuracy. Only under these conditions does it make sense to construct a calibration curve $I_1/I_2 = f(S_1/S_2)$ for further use for analytical purposes. Studies of this sort have not yet been performed.

Study of the secondary ion emission spectrum may prove promising for qualitative, and possibly even quantitative, determinations of minor impurities in metals. A certain picture of the possibilities of the secondary ion emission method is given by a preliminary investigation made in the laboratory of the present author. A steel ribbon of the following impurity content was studied: $C = 0.39\%$, $Mn = 0.45\%$, $Cr = 0.28\%$, $P = 0.016\%$, $Si = 0.01\%$. The secondary ion emission mass spectrum showed the following ions involving the presence of the impurities in the iron: C^+, C^-, C_2^-, C_4^-, Mn^+, MnO^+, MnO^-, Cr^+, $Cr_2O_3^+$, P^-, PO_2^-, PO_3^-, and Si^-.* The determination of carbon in iron presents difficulty, since the ions C^+, C_2^-, and C_4^- are also sputtered from molecules of hydrocarbons adsorbed on the surface of the iron. As for all the other impurities, their characteristic ions appeared in the mass spectrum. Thus we can consider the possibility proved of detecting them qualitatively by the secondary ion emission method. However, we should note that the intensities of the impurity ion beams do not correspond to their content in the target material, owing to the great differences between their sputtering coefficients. Thus, for example, the studied steel ribbon contained a relatively great content of chromium and a small one of phosphorus. However, the Cr^+ ion beam intensity was small, while that of P^- ions was considerably greater.

We can refer to still another experiment characterizing the possibilities of the secondary ion emission method from the standpoint of detecting impurities. A thin selenium film evaporated on a glass support was studied. The selenium contained copper in the amount $3 \times 10^{-4}\%$. The mass spectrum of the target showed ion beams of the isotopes of copper. An ion current of $^{63}Cu^+ \sim 10^{-14}$ A was measured under the conditions stated above. If the $^{63}Cu^+$ ion current were measured with an ion counter,[67] it should be possible to detect a copper impurity in selenium at a concentration at least four orders of magnitude smaller. This example shows that the secondary ion emission method, with appropriate development, can be applied to analyze for impurities in ultrapure metals and semiconductors.

The secondary ion emission method can also be applied for isotopic analysis of samples. Its possibilities along this line have been studied in[26 68].

---

*The ion $^{28}Si^+$ cannot be distinguished from the ions N_2^+ and CO^+ of the same mass. A negative ion of mass 28 can belong only to silicon, since the ions N_2^- and CO^- are not stable.[66]

CONCLUSION

Although the study of the phenomenon of secondary ion emission is just beginning, and extensive and systematic studies of the phenomenon itself are still necessary to establish its laws and to construct a theory of it, important possibilities have appeared, even at this stage, of using this phenomenon in various fields of physics and physical chemistry. The application of the phenomenon of secondary ion emission to study such processes as adsorption, catalysis, and gaseous corrosion is especially important. The possibility is not ruled out that new fields of application of this phenomenon will be found upon deeper study of secondary ion emission.

All this permits us to hope that the next few years will be a time of intensive study of the phenomenon discussed in this article.

[1] F. L. Arnot, Nature 138, 162 (1936).

[2] F. L. Arnot and J. O. Milligan, Proc. Roy. Soc. London A156, 538 (1936).

[3] F. L. Arnot, ibid. A158, 137 (1937).

[4] F. L. Arnot, ibid. A158, 157 (1937).

[5] F. L. Arnot and C. Beckett, Nature 141, 1011 (1938).

[6] F. L. Arnot and C. Beckett, Proc. Roy. Soc. London A168, 103 (1938).

[7] R. H. Sloane and R. Press, Proc. Roy. Soc. London A168, 284 (1938).

[8] V. L. Granovskiĭ, Élektricheskiĭ tok v gaze (Electric Current in a Gas), Gostekhizdat, M.-L., 1952.

[9] H. S. W. Massey and E. H. S. Burhop, Electronic and Ionic Impact Phenomena, Clarendon Press, Oxford, 1952.

[10] Ja. M. Fogel, B. T. Nadicto, V. F. Ribalko, R. P. Slabospitsky, I. E. Korobchanskaja, and V. I. Shvachko, J. Catalysis 4, No. 2, 153 (1965).

[11] V. I. Veksler and G. N. Shuppe, ZhTF 23, 1573 (1953).

[12] V. I. Veksler and M. B. Ben'yaminovich, ZhTF 26, 1671 (1956), Soviet Phys. Tech. Phys. 1, 1626 (1956).

[13] I. M. Mitropan and V. S. Gumenyuk, JETP 32, 214 (1957), Soviet Phys. JETP 5, 157 (1957).

[14] I. M. Mitropan and V. S. Gumenyuk, JETP 34, 235 (1958), Soviet Phys. JETP 7, 162 (1958).

[15] B. V. Panin, JETP 41, 3 (1961), Soviet Phys. JETP 14, 1 (1962).

[16] V. Walther and H. Hintenberger, Z. Naturforsch. 18a, 843 (1963).

[17] Ya. M. Fogel', R. P. Slabospitskiĭ, and A. B. Rastrepin, ZhTF 30, 63 (1960), Soviet Phys. Tech. Phys. 5, 58 (1960).

[18] B. M. Batanov, FTT 3, 642 (1961), Soviet Phys. Solid State 3, 471 (1961).

[19] B. M. Batanov, FTT 4, 1778 (1962), Soviet Phys. Solid State 4, 1313 (1963).

[20] R. E. Honig, J. Appl. Phys. 29, 549 (1958).

[21] R. C. Bradley, J. Appl. Phys. 30, 1 (1959).

[22] R. C. Bradley, A. Arking, and D. S. Beers, J. Chem. Phys. 33, 764 (1960).

[23] Ya. M. Fogel', R. P. Slabospitskiĭ, and I. M. Karnaukhov, ZhTF 30, 824 (1960), Soviet Phys. Tech. Phys. 5, 777 (1961).

[24] R. C. Bradley and E. Ruedl, J. Appl. Phys. 33, 880 (1962).

[25] V. E. Krohn, Jr., J. Appl. Phys. 33, 3523 (1962).

[26] J. Guepin, Theses, Paris, Centre d'Orsay, 1963.

[27] J. A. McHugh and J. C. Sheffield, J. Appl. Phys. 35, 512 (1964).

[28] Ya. M. Fogel', B. T. Nadykto, V. I. Shvachko, and V. F. Rybalko, Zhur. Fiz. Khim. 38, 2397 (1964).

[29] Ya. M. Fogel', R. P. Slabospitskiĭ, and A. S. Slavnyĭ, Radiotekhnika i elektronika 8, 684 (1963).

[30] Ya. M. Fogel', B. T. Nadykto, V. F. Rybalko, R. P. Slabospitskiĭ, I. E. Korobchanskaya, and V. I. Shvachko, Kinetika i kataliz 5, 154 (1964), Kinetics and Catalysis 5, 127 (1964).

[31] V. I. Shvachko, B. T. Nadykto, Ya. M. Fogel', and K. S. Garger, DAN SSSR 161, 886 (1965).

[32] V. I. Shvachko, B. T. Nadykto, Ya. M. Fogel', B. M. Vasyutinskiĭ, and G. N. Kartmazov, FTT 7, 1944 (1965), Soviet Phys. Solid State 7, 1572 (1966).

[33] D. T. Goldman and A. Simon, Phys. Rev. 111, 383 (1958).

[34] R. Bernard, R. Goutte, C. Guillaud, and R. Javelas, Compt. rend. 253, 1047 (1961).

[35] V. I. Veksler, JETP 38, 324 (1960), Soviet Phys. JETP 11, 235 (1960).

[36] R. Goutte, Theses, Lyon, 1959.

[37] L. P. Levine and H. W. Berry, Phys. Rev. 118, 158 (1960).

[38] H. E. Stanton, J. Appl. Phys. 31, 678 (1960).

[39] B. V. Papin, JETP 42, 313 (1962); Soviet Phys. JETP 15, 215 (1962).

[40] F. Kirchner and A. Benninghoven, Phys. Letts. 8, 193 (1964).

[41] A. Benninghoven, Ann. Physik 15, 113 (1965).

[42] U. A. Arifov, A. Kh. Ayukhanov, V. A. Shustrov, R. M. Khasanov, and V. I. Poltoratskiĭ, DAN SSSR 155, 306 (1964), Soviet Phys. Doklady 9, 214 (1964).

[43] R. I. Garber and A. I. Fedorenko, UFN 83, 385 (1964), Soviet Phys. Uspekhi 7, 479 (1965).

[44] C. Brunee, Z. Physik 147, 161 (1957).

[45] M. A. Eremeev, DAN SSSR 79, 775 (1951).

[46] U. A. Arifov and A. Kh. Ayukhanov, Izv. AN SSSR, ser. Fiz. 20, 1165 (1956), Bull Acad. Sci. Phys. Ser. 20, 1057 (1956).

[47] Ya. M. Fogel', A. G. Koval', Yu. Z. Levchenko, and A. F. Khodyachikh, JETP 39, 548 (1960), Soviet Phys. JETP 12, 384 (1960).

[48] D. V. Pilipenko and Ya. M. Fogel', JETP 48, 404 (1965); Soviet Phys. JETP 21, 266 (1965).

[49] R. Bernard, R. Goutte, C. Guillaud, and R. Javelas, Electron Microscopy Conference, Philadelphia, 1962, Vol. 1, p. C-7.

[50] V. I. Veksler, Izv. AN Uzb. SSR, No. 4, 34 (1959).

[51] Ya. M. Fogel', B. T. Nadykto, V. F. Rybalko, V. I. Shvachko, and I. E. Korobchanskaya, Kinetika i Kataliz 5, 496 (1964).

[52] Ya. M. Fogel', B. T. Nadykto, V. I. Shvachko, V. F. Rybalko, and I. E. Korobchanskaya, DAN SSSR 155, 171 (1964).

[53] Ya. M. Fogel', B. T. Nadykto, V. I. Shvachko, V. F. Rybalko, and I. E. Korobchanskaya, Kinetika i Kataliz 5, 943 (1964).

[54] V. I. Shvachko and Ya. M. Fogel', ibid. 7, 722 (1966).

[55] V. I. Shvachko, Ya. M. Fogel', and V. Ya. Kolot, ibid. 7, 834 (1966).

[56] M. I. Temkin and S. L. Kiperman, Zhur, Fiz. Khim. 20, 151 (1946).

[57] J. Horiuti and N. Takezawa, J. Res. Inst. Catalysis Hokkaido Univ. 8, 170 (1961).

[58] M. I. Temkin, N. M. Morozov, and E. N. Shalatina, Kinetika i Kataliz 4, 260 (1963); Kinetics and Catalysis 4, 224 (1963).

[59] M. I. Temkin, N. M. Morozov, and E. N. Shalatina, ibid. 4, 565 (1963); Kinetics and Catalysis 4, 494 (1963).

[60] M. I. Temkin, in collected volume Nauchnye osnovy podbora i proizvodstva katalizatorov (Scientific Bases of Selection and Production of Catalysts), pp. 46–67, Novosibirsk, 1964.

[61] G. K. Boreskov, Kinetika i Kataliz 6, 366 (1965).

[62] L. L. Barnes, Phys. Rev. 42, 487 (1932).

[63] R. Bernard and R. Goutte, Compt. rend. 246, 2597 (1958).

[64] R. Castaing and G. Slodzian, Compt. rend. 255, 1893 (1962).

[65] R. Castaing and G. Slodzian, Radiotekhnika i élektronika 10, 348 (1965).

[66] Ya. M. Fogel', V. F. Kozlov, and A. A. Kalmykov, JETP 36, 1354 (1959); Soviet Phys. JETP 9, 963 (1959).

[67] V. F. Kozlov, V. Ya. Kolot, and A. N. Dovbnya, PTE 6, 81 (1965).

[68] F. A. White, J. C. Sheffield, and F. M. Rourke, J. Appl Phys. 33, 2915 (1962).

Translated by M. V. King